Diploma Thesis

Stabilization of a He-Ne Laser

Andreas Pfennich

Institute of Electrical Measurement and Measurement Signal Processing
Graz University of Technology
Head of the Institute: Univ.-Prof. Dr. Georg Brasseur

Supervisor: Dipl.-Ing. Dr. techn. Markus Brandner

July 2012

Kurzfassung

Die hochauflösende optische Verschiebungsmessung ist eines der Forschungsgebiete am Institut für elektrische Messtechnik und Messsignalverarbeitung. Auflösungen im Nanometerbereich werden durch die Verwendung von Michelson Interferometern erreicht welche auf dem Prinzip der Interferenz von zwei kohärenten Lichtstrahlen beruhen. Interferometer übersetzen den Wegunterschied zwischen einem festen Referenzarm und einem Messarm in ein Interferenzsignal. Dabei dient die Wellenlänge der Lichtquelle als Referenz. Folglich bildet eine stabile Lichtquelle die Grundlage für Verschiebungsmessungen mit geringer Messunsicherheit.
Diese Arbeit befasst sich mit dem Design, der Implementierung und der experimentellen Verifikation einer autonomen, stabilisierten Helium Neon Laserquelle für den Einsatz in einem Michelson Interferometer. Im theoretischen Teil dieser Arbeit werden die Anforderungen an eine solche Laserquelle analysiert und verschiedene Methoden zur Stabilisierung von Helium Neon Lasern diskutiert. Der praktische Teil dieser Arbeit beschreibt die benötigten Experimente, zur Bestimmung der Eigenschaften verschiedener Helium Neon Laserröhren und das Design einer Regelstrategie. Des Weiteren werden das Design und die Implementierung von Hardware und Software Modulen präsentiert, welche für die Stabilisierung der Laserquelle benötigt werden. Die Arbeit schließt mit der experimentellen Verifikation der realisierten Laserquelle und diskutiert mögliche zukünftige Verbesserungen.

Abstract

Highly resolving optical displacement measurement is one area of research at the Institute of Electrical Measurement and Measurement Signal Processing. Nanometer resolution is achieved using Michelson interferometers that are based on the principle of interference of two coherent light beams. Interferometers translate the path difference between a fixed reference arm and a measurement arm into an interference signal using the wavelength of the light source as a reference. Consequently, a stable light source provides the basis for any low uncertainty displacement measurement.
This thesis is concerned with the design, implementation, and experimental validation of a standalone stabilized Helium Neon laser source for the use in a Michelson interferometer setup. In the theoretical part of this thesis the requirements for the laser source are analyzed and different approaches to the stabilization of Helium Neon lasers are discussed. The practical part of this thesis describes the experiments required to determine the properties of different Helium Neon laser tubes and consequently the design of a control strategy. Furthermore, the design and implementation of the hardware and software modules required to stabilize the laser source are presented. The thesis concludes with the experimental validation of the constructed standalone laser source and a discussion of possible future improvements.

Statutory Declaration

I declare that I have authored this thesis independently, that I have not used other than the declared sources / resources, and that I have explicitly marked all material which has been quoted either literally or by content from the used sources.

Place	Date	Signature

Contents

1 Introduction

Arthur L. Schawlow, one of the inventors of the laser, once said "The Laser is a solution in search of a problem". This was in the early nineteen sixties shortly after the first laser produced coherent light. Back then nobody could think of the endless applications a laser is suited for.
Today the laser is an indispensable tool in many applications. In industry and medicine, high power lasers are used for material processing and the ablation of tissue. Modern communication uses lasers for high speed data transfer. Lasers are also used in optical metrology to measure for example distances, surface deformations, velocities in fluid flows, or vibrations. Such measurement methods have the advantages of contact free measurement and high resolution.

1.1 Motivation

Optical metrology is one area of research at the Institute of Electrical Measurement and Measurement Signal Processing (EMT). Most of the ongoing theses in this area have the focus on high resolution optical displacement measurement.

Figure 1.1 shows the basic principle of a Michelson Interferometer (MI) for displacement measurement. One coherent light beam from a laser source hits a Non Polarizing Beam Splitter (NPBS) and is split into two beams. One beam goes into the reference path of the MI and hits a fixed reference reflector. The other beam, however, travels along the measurement path and hits the measurement reflector. Both beams are reflected and recombined by the NPBS. They impinge on a single detector.
If the measurement mirror is not in motion, the intensity on the detector is constant. But in case of a moving measurement mirror, the intensity on the detector changes between zero and its maximum. This is the result of constructive and destructive interference. One cycle of the intensity change equals a displacement of half the wavelength λ of

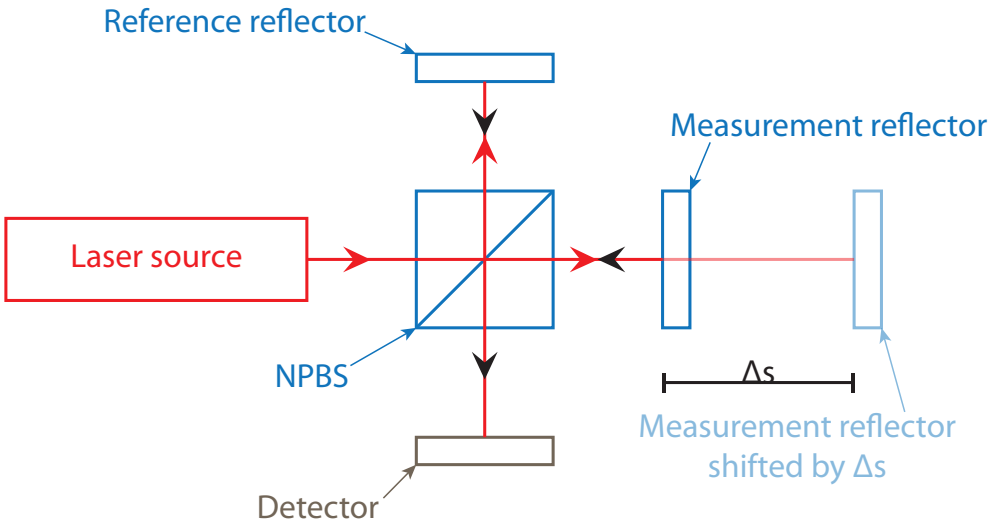

Figure 1.1: Schematic assembly of a MI with all its components necessary to detect the displacement Δs. (Similar to [4].)

the coherent light from the laser source. If we count the transitions between zero and maximum intensity N we can express the displacement by

$$\Delta s = \frac{\lambda}{2} N. \tag{1.1}$$

It is evident that the wavelength and, therefore, the frequency of the coherent light is crucial for the measurement.

In the course of developing a White Light Interferometer for high resolution, non-contact surface measurement, Auer [4] developed a miniaturized MI to measure displacements, for which Kern [17] developed the signal processing. Auer chose the homodyne detection method for his MI, which requires Linearly Polarized (LP) coherent light with one frequency. Another detection method for a MI is heterodyne detection, which requires a laser source that produces coherent light with two orthogonally LP frequencies [7].

1.2 Problem Description and Requirements

The goal of this thesis is the construction of a stabilized He-Ne laser source for the use in either a heterodyne or homodyne MI. Therefore, the emitted coherent light of the stabilized He-Ne laser source has to be orthogonally LP with two frequencies. The second criteria is that the frequencies are as stable as possible, because variations result in

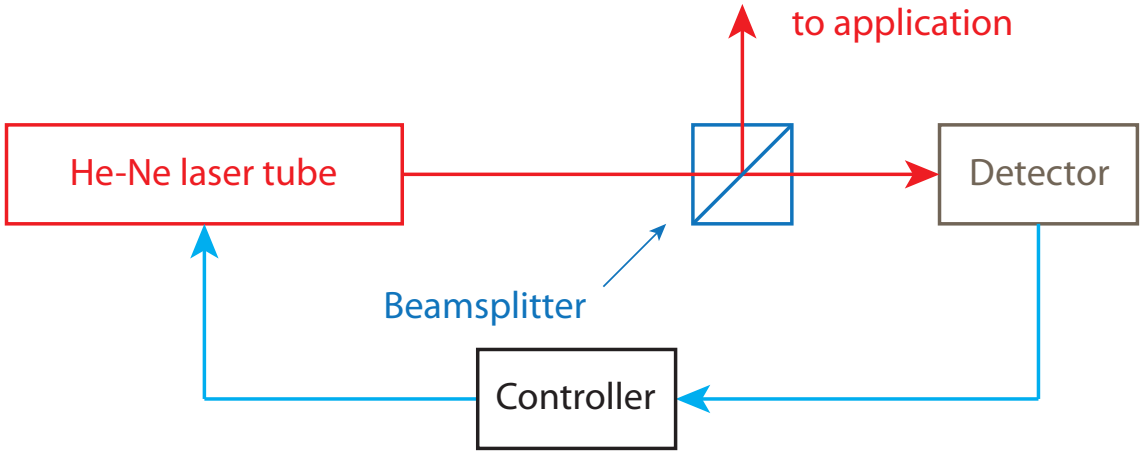

Figure 1.2: Basic principle of stabilizing a Helium Neon (He-Ne) laser tube. The coherent light is directed to the application and the detector. The controller uses the detector signal to keep the length of the He-Ne laser tube constant.

higher measurement uncertainties [4]. This task has to be accomplished by using a He-Ne laser tube already existing at the EMT.

Without modifications whatsoever He-Ne laser tubes generate Non Polarized (NP) coherent light with multiple frequencies within a certain bandwidth. The main reason for this variation is that the frequencies of the emitted coherent light depend on the laser tube length. Minimal changes in the length of the laser tube will result in very high frequency variations. Therefore, we have to find a method to characterize the frequency variations and use this information to stabilize the length of the laser tube. Figure 1.2 shows the basic approach to stabilize a He-Ne laser tube. This control method has to be easy enough to implement and suited for practical applications.

Before constructing the stand alone stabilized He-Ne laser source we test the concept itself and the applicability of the existing He-Ne laser tubes using an experimental set-up. Finally the stability of the frequencies of the coherent light emitted by the stabilized laser source has to be validated. Requirements for the prototype are:

- The underlying light source has to be an already existing He-Ne laser tube with its power supply.
- The control algorithm must allow the stabilized laser tube to produce coherent light with two orthogonally LP frequencies .
- Because this standalone stabilized He-Ne laser source is also used for teaching purposes it shall be possible to acquire the control variable with a Data Acquisition System (DAQ) and use a Personal Computer (PC) as an external controller.

- The standalone stabilized He-Ne laser source has to possess an indication whether the frequency of the emitted coherent light is stable or not.
- The housing of the standalone stabilized He-Ne laser source must accommodate the He-Ne laser tube, the detection unit, the controller, the interface, and the whole power supply. Furthermore, it must be possible to disassemble and reassemble the prototype with little effort.

2 Fundamentals

The concern of this chapter is to provide the theoretical background of the work presented in this thesis. It explains the physics behind a laser source, the principle of optical amplification using an optical cavity, and the reason why the frequency of the generated coherent light varies within a certain bandwidth. Furthermore, it discusses methods to stabilize a He-Ne laser tube. The last subject of this chapter is the analysis of frequency stability.

2.1 Physics of Coherent Light Generation

Light emitted by a laser has the following properties.

- **Monochromatic wave** - small bandwidths of the light waves
- **Coherence** - fixed spatial and temporal phase relationship between light waves
- **Small divergence** - light waves are highly directional
- **High power and energy densities**

This section aims to give a brief insight in how light with these properties is generated. Furthermore, it explains the need for optical cavities and explains some of their characteristics. And finally it describes the He-Ne laser tubes in particular. For more detailed information the reader is referred to [10] and [30].

2.1.1 Laser Principle

The term laser is an abbreviation for **L**ight **A**mplification by **S**timulated **E**mission of **R**adiation and stands for the underlying principle used to produce coherent light. Normally atoms of a certain active laser medium or so called gain medium are located in the

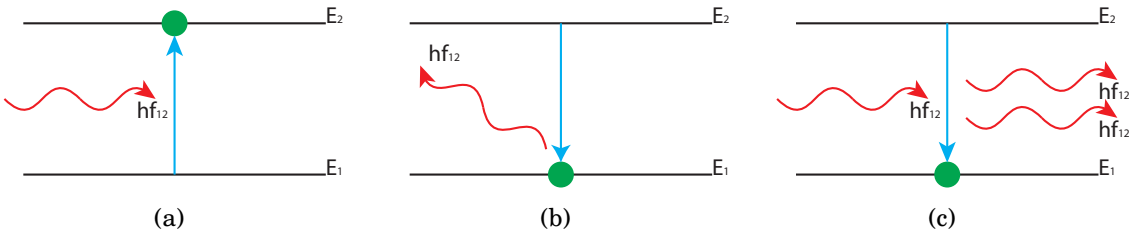

Figure 2.1: An atom is ascended into a higher energy level by the absorption of a photon (a). After a certain period of time an atom located on a higher energy level falls back on a lower energy level thus emitting a photon in a random direction (b). Under the influence of a photon an atom may fall down on a lower energy level, emitting a photon in the same direction (c).

lowest energy level E_1. If light with the frequency f_{12} hits an atom, the atom may ascend into a higher energy level E_2. That is when this equation

$$\Delta E = E_2 - E_1 = h f_{12}, \tag{2.1}$$

where h is the Plank constant is satisfied. A photon is removed from the light, therefore, reducing its intensity. This process is called absorption (figure 2.1(a)). On the other hand, atoms which are located in a higher energy level E_2 fall after a certain period of time back on the lower level E_1. This emits a photon with the frequency f_{12} in a random direction. This is called spontaneous emission (figure 2.1(b)). An atom, which is on a higher energy level E_2, may fall back on the lower level E_1 under the influence of light, with the frequency f_{12}. Thus emitting a photon with the same frequency, phase, and direction, this is called the stimulated emission (figure 2.1(c)). The intensity of the light is amplified. This amplification is only possible if the density of atoms in higher energy levels is grater than the density in lower ones, i.e.

$$N_2 > N_1. \tag{2.2}$$

Such a state is called population inversion. And it is achieved, depending on the gain material, by pumping either optical, electrical, or chemical energy into the gain material.

In theory the energy levels E_1 and E_2 are well defined and absorption or emission of light happens with only one frequency f_{12}. But there are numerous physical effects or so called line broadening mechanisms, which are responsible for uncertainties in the energy levels E_1 and E_2. These line broadening effects are, therefore, responsible that the frequency of the emitted coherent light is within a certain bandwidth, depicted in figure 2.2(a). Those line broadening mechanisms are either homogeneous or inhomogeneous. Homogeneous

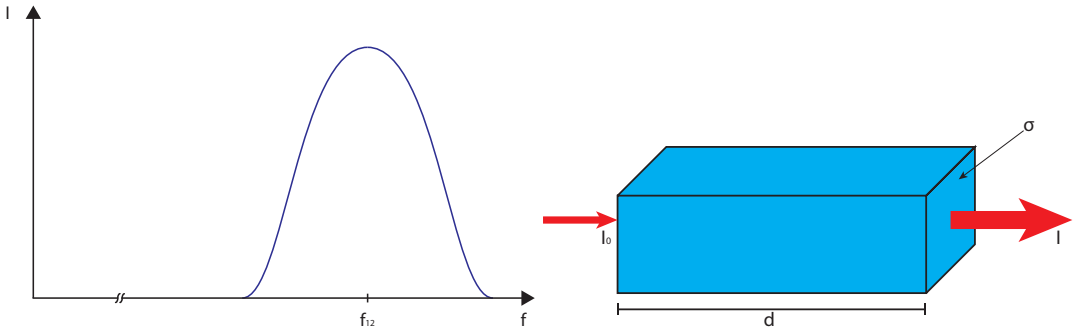

(a) (b)

Figure 2.2: A typical gain curve is depicted in (a), it plots the intensity of the generated coherent light versus its frequency. The bandwidth and the position of the gain curve depends on the gain medium. However, (b) depicts the amplification of light through a certain excited gain medium as it is expressed in equation 2.3.

mechanisms effect all atoms equally. Examples are the natural line-width or elastic collision of the atoms. Inhomogeneous mechanisms, however, effect all atoms differently like the Doppler-broadening or broadening through the Stark-effect. The shape of the gain curve depends on the line broadening mechanism which depends on the gain medium [10].

2.1.2 Optical Cavities

In a laser atoms of a gain medium are ascended into higher energy levels by pumping energy into a gain medium. The incident light is amplified by stimulated emission, thus producing coherent light within a certain bandwidth. The equation

$$G = \frac{I}{I_0} = \exp(\sigma(N_2 - N_1)d) \tag{2.3}$$

gives a relation between gain G, incident light intensity I_0, transmitted light intensity I, thickness d, and the absorption cross section σ of the gain medium [10]. Figure 2.2(b) shows the incident light which is amplified through a excited gain medium.
In the most gain materials the gain is too small to produce coherent light with sufficient intensity. To increase the gain two mirrors one Highly Reflecting (HR) and one partially transmitting, are placed on each side of the gain medium as depicted in figure 2.3. This assembly is called an optical cavity. By multiple runs through the gain medium the light experiences a higher amplification. Thus creating an almost plane and coherent light wave. That is when the gain (equation 2.3) is high enough to compensate for the losses.

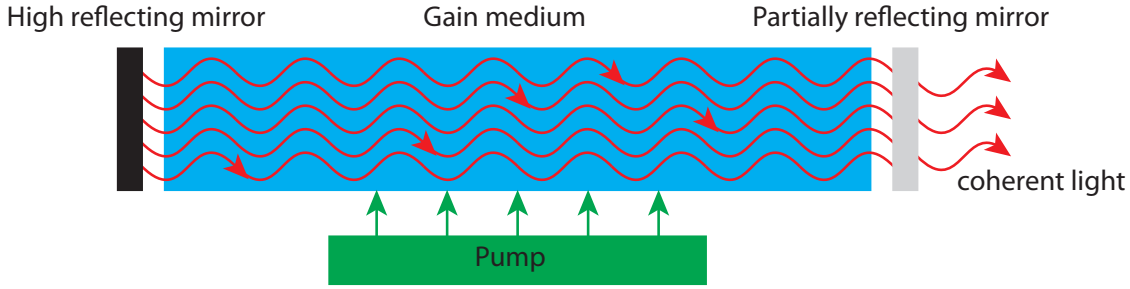

Figure 2.3: Energy is pumped into the gain medium thus creating population invasion which is a prerequisite for creating coherent light. A standing wave is formed between the HR and partially reflecting mirror. The standing wave leaves the optical cavity through the partially reflecting mirror.

This is characterized in the threshold condition [10]

$$GRT < 1, \tag{2.4}$$

where R is the geometric mean of the reflectance of the two mirrors. And T is the transmittance which states other losses, such as losses through diffraction or dispersion. The light waves reflected in the optical cavity take the form of standing waves or so called axial modes. That is if the length of the optical cavity L is an integer multiple m of the half of the wavelength [14], i.e.

$$L = m\frac{\lambda_m}{2} \qquad m \in \mathbb{N}. \tag{2.5}$$

The frequency $f_m = \frac{c}{\lambda_m}$, where c is the velocity of light of a single axial mode is, therefore,

$$f_m = m\frac{c}{2L} \tag{2.6}$$

and the difference frequency between two axial modes or Free Spectral Range (FSR) is

$$FSR = f_{m+1} - f_m = \frac{c}{2L}. \tag{2.7}$$

If we plot these axial modes into the gain curve of figure 2.2(a), as done in figure 2.4, we can see that only a few axial modes fit under the gain curve and fewer are above the laser threshold (equation 2.4). These are the axial modes of the coherent light which are amplified and, therefore, emitted by the laser. The intensity of each axial mode corresponds to its position on the gain curve. And, therefore, is the overall intensity of the emitted coherent light the sum of the intensities of each axial mode, which are above

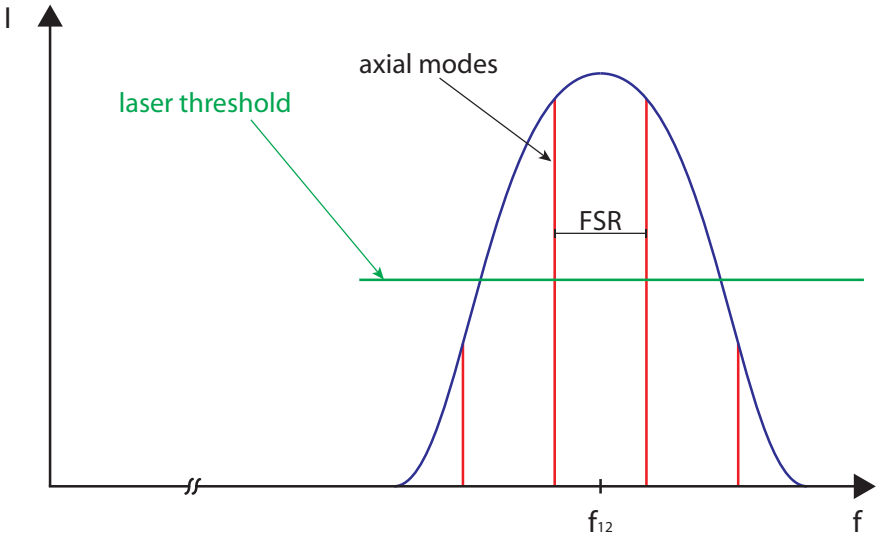

Figure 2.4: A typical gain curve superimposed with the axial modes of the optical cavity. The two axial modes above the laser threshold have equal intensity and a fixed FSR. The intensity of the coherent light emitted by the laser is the sum of the intensities of the axial modes. The frequencies of the axial modes are the frequencies of the coherent light.

the laser threshold and under the gain curve. It is apparent that the number of axial modes which are amplified depends on the length of the optical cavity. A longer optical cavity results in more axial modes and, therefore, a smaller FSR. In addition to that, the frequencies of the axial modes also depend on the optical cavity's length.
Variations in the length of the optical cavity result in variations in the frequencies of the coherent light emitted by the laser. Such length variations can occur through changes in the temperature of the laser or ambient air, in pressure changes of the ambient air, or mechanical vibrations. These frequency changes are associated with intensity changes.

2.1.3 He-Ne Laser Tubes

The He-Ne laser tube is a very simple and reliable laser with a long lifetime [19]. Its gain medium is a Helium-Neon gas mixture and, therefore, it belongs to the family of gas lasers. Figure 2.5 shows the schematic cross section of a He-Ne laser tube. Basically the laser consists of a glass tube filled with the He-Ne gas mixture, a cathode and an anode, a glass capillary, and two mirrors one HR and one partially transmitting, which forms the optical cavity.
The laser transition happens in the neon atoms. By feeding a high voltage ($V_{in} \sim 2\,\mathrm{kV}$) to cathode and anode, the resulting electron discharges excite the helium atoms. Those

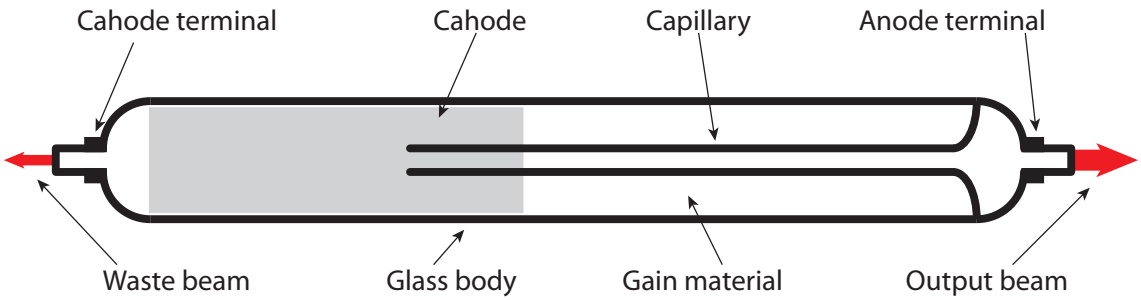

Figure 2.5: Schematic cross section over a He-Ne laser tube. It shows all the necessary elements to produce coherent light. The output beam exits the partially reflecting mirror, and the waste beam exits the HR mirror.

excited helium atoms then pass their energy through collisions to the neon atoms, which then fall down on lower energy levels thus emitting photons. The He-Ne laser tube is capable depending on its gas mixture and the presence of frequency selective elements in the optical cavity to emit coherent light with different wavelengths. All He-Ne laser tubes used in this thesis emit coherent light with the wavelength of $\lambda_{12} \sim 633\,\text{nm}$. This wavelength corresponds to a frequency of $f_{12} \sim 473.61\,\text{THz}$.
The capillary has a diameter around 1 mm and the electron discharge happens in it. Therefore, its diameter corresponds to the beam diameter. The mirrors of the optical cavity are directly connected to the class body of the tube. Although one mirror is said to be a HR mirror it is not 100 % reflecting and, therefore, also partially transmitting. For this reason the He-Ne laser emits coherent light on both ends of the tube. The beam exiting the HR mirror is called the waste beam and has a much lower intensity than the beam exiting the output mirror, which is called the output beam. Changes in intensity and, therefore, in frequency affect both beams alike.

In a He-Ne laser tube as in most gas lasers the main line broadening mechanism is the Doppler broadening. Under low pressures we can neglect other broadening mechanisms [10]. The Doppler broadening is caused by the random velocity of the moving atoms. The Doppler broadened gain curve is basically Gaussian shaped and its Full Width at Half Maximum (FWHM) depends on the temperature and the mass of the atoms. For a He-Ne laser tube the FWHM is approximately 1500 MHz [10]. Depending on the length of the optical cavity, the He-Ne laser tube emits either one or several axial modes. Each axial mode tends to be orthogonally LP to the adjacent one and has a fixed direction of polarization [13].

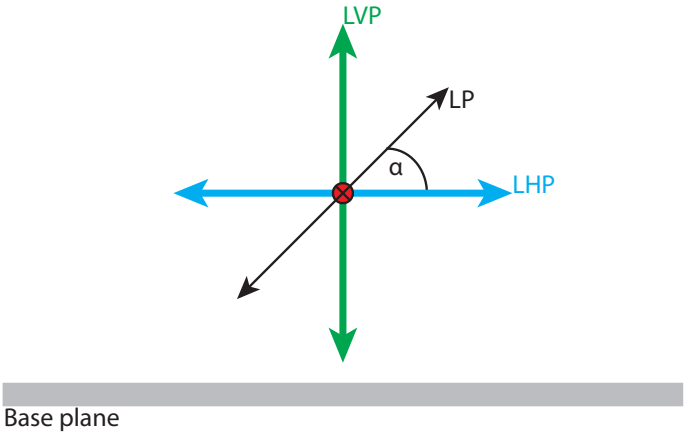

Figure 2.6: The polarization of the axial modes are perpendicular (LVP) and parallel (LHP) to the base plane. Any tilt in the polarization of a axial mode or an optical component is expressed with the angle α. The propagation direction of the axial modes is into the plane of projection.

2.2 Laser Frequency Stabilization

We know that the frequencies of the coherent light emitted by a laser source correspond to the frequencies of the axial modes. And that changes in the length of the optical cavity are the reasons for uncertainties in the frequencies of the axial modes (equation 2.6). The underlying principle of all stabilization methods is the comparison between the frequencies of the axial modes and a stable reference. This information is used to generate a control variable for a controller which stabilizes the length of the optical cavity. This happens by either thermal stabilization, a piezoelectric crystal attached to one of the mirrors of the optical cavity, or by a combination of both methods. The most sophisticated methods were introduced by Hansch and Couillaud [12], and Drever *et al.* [9] which both use a reference optical cavity. Another sophisticated approach uses the saturated absorption in iodine vapour [38]. Those methods achieve the highest frequency stability, but are also very complex and, therefore, not suited for our application.

The following section discusses the three basic methods [7] used in industry to stabilize a He-Ne laser tube so that it emits coherent light with two frequencies. We compare the methods regarding the complexity of the required optical assembly.

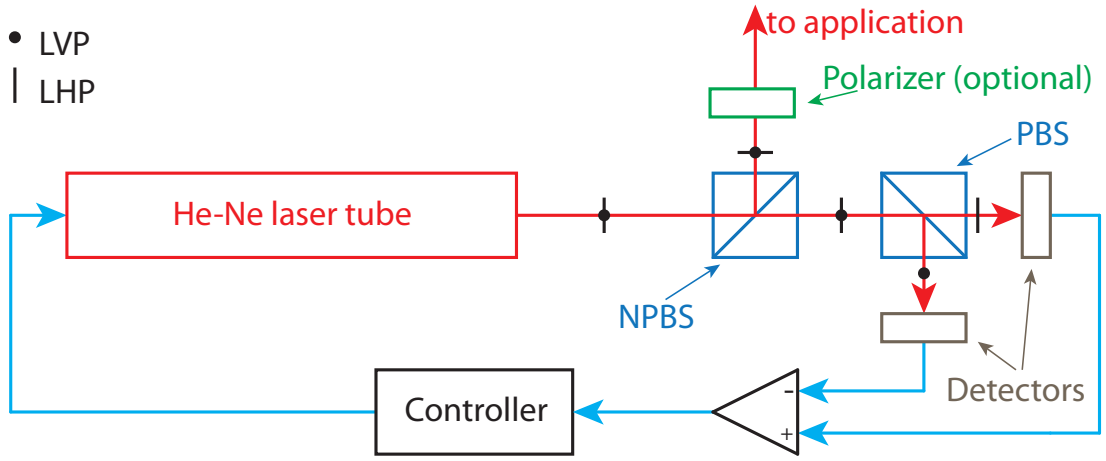

Figure 2.7: Basic assembly of a dual mode He-Ne laser tube stabilized using the comparison of axial mode method [6]. The controller changes the length of the He-Ne laser tube so that the intensities of the LHP and LVP axial modes are equal.

2.2.1 Comparison of Axial Modes

One method to produce coherent light with two stable frequencies, is the comparison of axial modes. The underlying light source for this method is a dual mode He-Ne laser tube. Therefore, the laser tube has to be sufficiently short (equation 2.7) so that only two axial modes fit under the gain curve and are above the laser threshold.
Starting from the knowledge that in a He-Ne laser tube each axial mode is orthogonally LP to its adjacent one, the laser tube has to be aligned so that its axial modes are perpendicular and parallel LP to the base plane. Figure 2.6 depicts such a state, from now on we will refer to such polarization states as Linearly Horizontally Polarized (LHP) and Linearly Vertically Polarized (LVP). Furthermore, we will express any tilt of either a polarization state or an optical component with the angle α.

Figure 2.7 shows the basic approach for the frequency stabilization using the comparison of axial modes method [6]. The emitted coherent light hits a NPBS, which directs one part of the coherent light to the application. The other part hits a Polarizing Beam Splitter (PBS) and is split according to the polarization states of its axial modes and fall on the detectors. These detectors produce an electrical signal proportional to the intensity of the incident axial modes. The difference of those signals is the control variable for the controller. Whose goal it is to control the length of the optical cavity so that both intensities are equal. This state is depicted in figure 2.4. One frequency operation is achieved by placing a polarizer between the NPBS and the application, to block either the LHP or LVP axial mode.

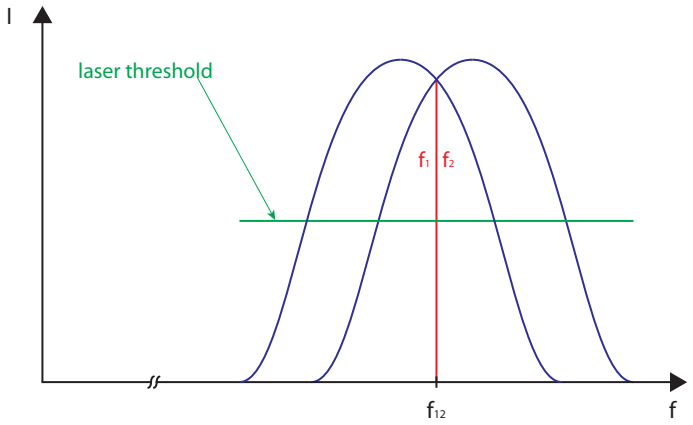

Figure 2.8: An axial magnetic field splits the Doppler broadened gain curve of the He-Ne laser tube into two components. The axial mode consists of two frequency components, one is LCP the other RCP. The two components have different frequencies. This arises because of different optical path lengths for each component, due to the Zeeman splitting [29].

The frequency difference archived with this method depends on the length of the optical cavity of the laser tube (equation 2.7). Typical values for a dual mode He-Ne laser tube are within a few hundred MHz. Note that although the length of the optical cavity changes, the frequency difference stays constant. The only crucial factor in this method is that the He-Ne laser tube is aligned so that the axial modes are LHP and LVP. If the laser tube is not aligned properly, the detector signals have an offset.

2.2.2 Axial Zeeman Laser

A widely used method to create coherent light with two orthogonally LP frequencies using a He-Ne laser tube is the so called Zeeman splitting, based upon the Zeeman effect.
An axial magnetic field applied to a single mode He-Ne laser tube causes the gain curve to split into two components, depicted in figure 2.8. The strength of the magnetic field determines the shift between the two gain curves [5]. Depending on the length of the optical cavity, a number of axial modes fit under the two gain curves. The intensity and frequency of each axial mode is again defined by its position on the gain curve.
When an axial mode is located on only one gain curve it is either Left Circularly Polarized (LCP) or when located on only the other gain curve Right Circularly Polarized (RCP). But when the axial mode is in the area where both gain curves overlap, it consists out of a LCP component and a RCP component. The intensity of each component is defined by its corresponding gain curve. Although both components are part of the same axial

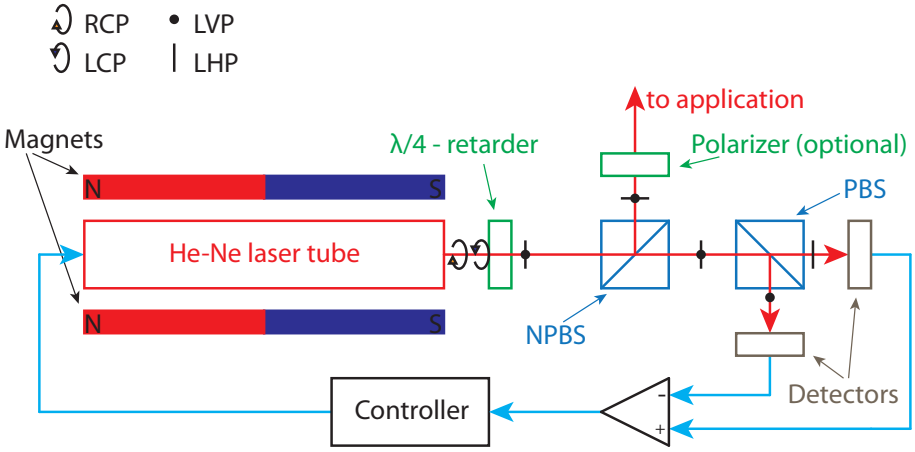

Figure 2.9: Basic assembly of a He-Ne single mode laser tube stabilized using Zeeman splitting [29]. An axial magnetic field applied to the laser tube, splits the axial mode into a LCP and RCP component. The controller changes the length of the He-Ne laser tube so that both LCP and RCP components of the same axial mode have the same intensity.

mode, they have different frequencies f_1 and f_2. This frequency difference arises because of different optical path lengths for the two polarization states in the optical cavity due to the Zeeman splitting [5]. The maximum frequency difference reached with this method is around 4 MHz [40][1].

Figure 2.9 shows a basic assembly of an axial Zeeman split dual frequency laser [29]. A single mode He-Ne laser tube is brought into an axial magnetic field. This is achieved by surrounding the laser tube with permanent magnets. The resulting LCP and RCP coherent light goes through a $\frac{\lambda}{4}$-retarder. Which turns when its fast axis is aligned at $\alpha = 45°$ RCP light into LHP light and LCP light into LVP light.
Then one part of the coherent light is reflected by the NPBS and goes to the application. The other part, however, is split by a PBS according to its polarization state. Each of the two resulting light beams fall on separate detectors, which produce an electrical signal proportional to the intensity of the incident coherent light. The difference of those two signals now form the control variable by which means the controller is able to stabilize the length of the optical cavity. The goal of the controller is to change the length of the optical cavity so that both components f_1 and f_2 of the axial mode have the same intensity. This state is depicted in figure 2.8. The emitted coherent light has now two stable frequencies with a fixed frequency difference. One frequency operation is achieved by placing a polarizer between the NPBS and the application, to block either the LHP or LVP component of the axial mode.

[1]This reference is no longer available on the Zygo website, but it is available on Sam's Laser FAQ [29]

Using this technique it is important to choose the length of the He-Ne laser tube and the strength of the magnetic field wisely. A longer optical cavity reduces the FSR between the axial modes (equation 2.7) and, therefore, more axial modes can fit under the split gain curve. This can lead to more than one axial modes which are amplified and, therefore, to more frequencies of the coherent light. A shorter optical cavity, however, results in a weaker overall intensity of the coherent light. Because the strength of the magnetic field is responsible for the shift in the gain curves, its strength has to be adjusted to the length of the tube. A stronger magnetic field can result in a greater shift and, therefore, more axial modes are amplified. For a more detailed description the reader is refereed to [29].

2.2.3 Acousto-Optic Modulator

With an Acousto Optic Modulator (AOM) it is not possible to stabilize the frequency of the coherent light generated by a He-Ne laser tube. It is rather used to split the incoming coherent light into two beams with an adjustable difference frequency.

An AOM is a transparent crystal with a piezoelectric transducer attached to it. This transducer excites a sound wave with a certain frequency, which changes the refractive index of the transparent crystal through mechanical pressure. This change of the refractive index causes the diffraction of some of the incoming coherent light. The other part of the incoming coherent light is transmitted. The direction and the frequency of the diffracted beam can be controlled via the frequency of the sound wave. The intensity ratio between the transmitted and diffracted coherent light, however, is controlled via the acoustic power of the sound wave [11]. The created frequency differences by using an AOM usually are around 20 MHz [40].

Figure 2.10 shows an approach to create a two frequency laser presented by Dirksen *et al.* [8]. The underlying light source is either an already stabilized single or dual mode He-Ne laser tube. The He-Ne laser tube is aligned, so that the polarization of the axial modes are at $\alpha = \pm 45°$. Using a dual mode He-Ne laser tube requires a linear polarizer to block one axial mode. The coherent light beam entering the first WSP is LP with $\alpha = 45°$. This WSP splits the incoming beam into two beams one LHP and the other LVP with equal intensities. Those beams now enter the AOM and get partially transmitted and diffracted. The transmitted beams (indicated by the dashed lines) have no importance. The frequencies of the diffracted beams, however, are shifted according to the frequency of the sound wave f_s. The second WSP is identical to the first one and recombines the two

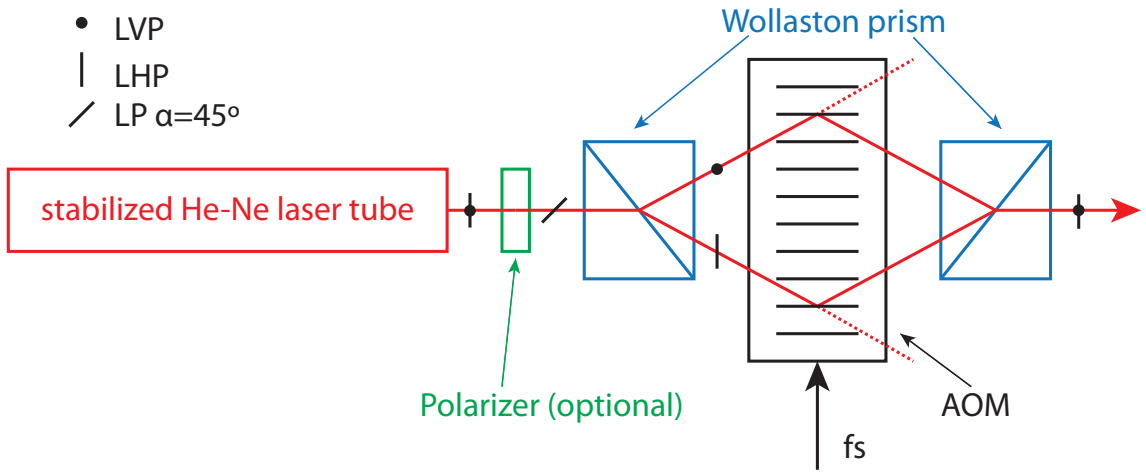

Figure 2.10: Basic assembly of one approach to create coherent light with two frequencies with the use of an AOM [8]. The LP axial mode is split by a Wollaston Prism (WSP) and diffracted by an AOM the recombined coherent light is LHP and LVP and has a difference frequency determined by the frequency driving the AOM.

diffracted beams. The frequency difference Δf achieved with this particular method is in a range of 1 MHz – 10 GHz and expressed by

$$\Delta f = 2 f_s. \tag{2.8}$$

The stability of the frequency difference depends on the frequency stability of the oscillator driving the AOM.

2.2.4 Comparison of Methods

This section we discuss the advantages and disadvantages of the previous described methods.

- The **comparison of axial mode** method creates a fixed difference frequency, determined by the length of the required dual mode He-Ne laser tube. The advantage of this method is that it is very simple to implement. Apart from the He-Ne laser tube and the electronics only a PBS is required.
- The **axial Zeeman laser** creates a tunable difference frequency, determined by the strength of the applied axial magnetic field. This method requires apart from the He-Ne laser tube and the electronics, a $\frac{\lambda}{4}$-retarder, a PBS, and magnets to create the magnetic field. This results in a complex assembly.

Method	Δf	Assembly complexity
Comparison of axial modes	Fixed $= FSR$	low
Axial Zeeman laser	Adjustable $\sim 4\,\mathrm{MHz}$	high
AOM	Adjustable 1 MHz - 10 GHz	very high

Table 2.1: The previous described methods are compared regarding their frequency difference Δf and the complexity of the required assembly.

- Using an **AOM** creates a tunable difference frequency, depending on the frequency of the oscillator driving the AOM. This method requires in addition to the AOM and the two WSP an already stabilized laser. Since such a laser has to be stabilized by one of the two previous described stabilization methods, using an AOM results in a very complex assembly.

Table 2.1 summarizes the introduced methods regarding their frequency difference and complexity of the assembly. Since the comparison of axial modes requires the least complex assembly we, therefore, chose it as stabilization method.

2.3 Frequency Comparison

Figure 2.11 depicts an overview of the approach we use to characterize the frequency stability of a laser source. The coherent light of two light sources falls on the same detector which produces an electrical signal with a frequency equivalent to the difference frequency of the two coherent light beams. The frequency is measured by a frequency counter and is then analyzed.

The following section briefly discusses the theoretical background of the approach we use to measure the frequency difference between the two coherent light beams. Furthermore, it discusses the way how this result is interpreted.

2.3.1 Optical Heterodyne Detection

The wave theory of light explains light as an transversal electromagnetic wave. This wave can be represented by the variation of its electrical field strength according to the following equation

$$E(t) = E_0 sin(2\pi f t), \tag{2.9}$$

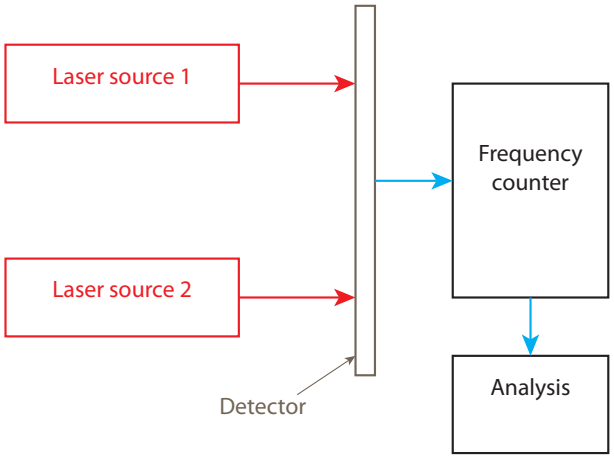

Figure 2.11: The frequency of the interference, created by the two coherent light beams, on the detector is measured with a frequency counter and is then analyzed.

where $E(t)$ is the electrical field strength with the amplitude E_0, f is the frequency, and t the time. Since the electric field oscillates with a few hundred THz it is not possible to measure its frequency directly. Instead it is only possible to measure the intensity, which is equivalent to the time average of the square of the electric field strength [10], i.e.

$$I = \langle E^2 \rangle_T \tag{2.10}$$

In optical heterodyne detection we align two beams of coherent light, one emitted by a reference laser source and the other emitted by our stabilized He-Ne laser tube. This leads to a superposition of the electric field strengths of the two light waves, i.e.

$$E = E_1 + E_2. \tag{2.11}$$

Using equation 2.10 the intensity of the interference of those two coherent light beams can be described by

$$I(t) = I_1 + I_2 + 2\sqrt{I_1 I_2}\cos(2\pi\delta f t). \tag{2.12}$$

The intensity on the detector has a frequency of $\delta f = f_1 - f_2$. This so called beat frequency can be measured easily using for example an oscilloscope. If we assume that the frequency stability of the reference laser source is much higher than the stability of our stabilized laser source, we can state that the variation in the beat frequency depends only on the variation of the stabilized laser source.

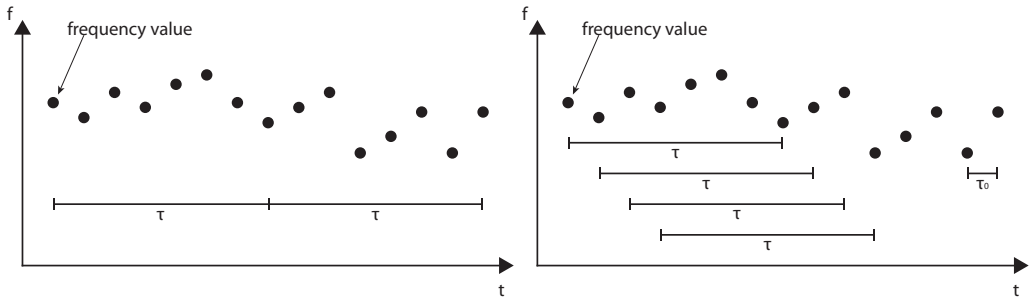

Figure 2.12: The Allan Variance (AVAR) averages the frequency values over a certain time interval τ (a). The overlapping AVAR uses overlapping sample sets to improve the confidence of the stability estimate (b). (Similar to [28].)

2.3.2 Allan Variance

To characterize the fluctuations of the beat frequency we use variances. The most prominent variance is the standard variance [28]

$$s^2 = \frac{1}{N-1}\sum_{i=1}^{N}(y_i - \overline{y})^2, \tag{2.13}$$

where the y_i are the N fractional frequency values and $\overline{y}$ is the average frequency. The standard variance gives a measure for the existing variation from the average. The standard variance is non convergent for some types of noise found in frequency sources, therefore, it is not recommended to use it as a measure for frequency stability [28].
Another way to express the frequency stability of a laser source is by the ratio between the maximum frequency variation and its mean frequency. This ratio is expressed in either parts per million (ppm) or parts per billion (ppb). This is done by most manufacturers of stabilized laser sources.

The AVAR gives a measure of the variation between one frequency value and the subsequent one. It is expressed by

$$\sigma_y^2(\tau) = \frac{1}{2(M-1)}\sum_{i=1}^{M-1}(y_{i+1} - y_i)^2, \tag{2.14}$$

where y_i is the ith of the M fractional frequency values averaged over the measurement interval τ (figure 2.12(a)). The AVAR contrary to the standard variance is convergent for most types of noise [28]. The square root of the AVAR is the Allan Deviation (ADEV) $\sigma_y(\tau)$.

To improve the confidence of the stability estimate it is necessary to use the so called overlapping AVAR expressed by

$$\sigma_y^2(\tau) = \frac{1}{2m^2(M-2m+1)} \sum_{j=1}^{M-2m+1} \left(\sum_{i=j}^{j+m-1} (y_{i+m} - y_i) \right)^2, \tag{2.15}$$

where M is the number of frequency measurements averaged over the interval $\tau = m\tau_0$. Where m is the averaging factor and τ_0 is the basic measurement interval (figure 2.12(b)). Again is the square root of the overlapping AVAR the overlapping ADEV.

Although there are many other variances, the overlapping AVAR is the most widely used and the first choice for frequency stability analysis. For much more detailed information about frequency stability analysis the reader is refereed to [28].

2.4 Summary

In the first part of this chapter we explain the laser principle and that the bandwidth of the emitted coherent light is created by numerous line broadening mechanisms. Furthermore, we state that the optical cavity is responsible for creating axial modes of which the emitted coherent light is composed of. The length of the optical cavity defines the frequency of the axial modes and, therefore, the frequencies of the emitted coherent light.
In the second part we discuss three different methods to stabilize a He-Ne laser tube. Those methods are, Zeeman splitting, comparison of axial modes, and the use of an AOM. We compare those methods and conclude that the axial modes method is the best choice because it requires the least complex assembly.
We give a brief insight of the method we use to validate the stability of our stabilized He-Ne laser tube. We state that it is only possible to compare the frequencies of two coherent light beams than to measure their frequencies directly. In the last section we discuss the methods to interpret the results of the frequency measurement. We state that the standard variance is only marginally suitable for expressing the frequency stability of our He-Ne laser tube. The first choice is the AVAR.

3 Commercial Laser Sources

In section 2.2 we explain the three most commonly used methods to stabilize a He-Ne laser tube. This chapter lists a few commercially distributed laser sources from three well known companies to give a brief insight in what is available on the market.

3.1 SIOS

The company SIOS Messtechnik GmbH is a German developer and manufacturer of laser interferometric systems. According to their product catalogue [32] they distribute two stabilized He-Ne laser sources, which both work with the comparison of axial mode method. Subsequent we list the main features of both systems, one is a two frequency laser (SL-02/2 [34]) and the other is a one frequency laser (SL-03 [33]).

SL-02/2

- The output power is $\geq 2.0\,\mathrm{mW}$.
- Two orthogonally LP frequencies with a difference frequency of $\Delta f = 730\,\mathrm{MHz}$.
- The frequency stability measured over one hour is $\pm 10\,\mathrm{ppb}$.

SL-03

- The output power is $\geq 0.8\,\mathrm{mW}$.
- One LP frequency.
- The frequency stability measured over one hour is $\pm 2\,\mathrm{ppb}$.

3.2 Agilent Technologies

Agilent Technologies is a major developer of measurement devices from California. They distribute numerous laser sources [1], all of them use the Zeeman splitting method for stabilization. The characteristics are listed as followed.

- The output power off all their systems is $\geq 0.12\,\mathrm{mW}$.
- Their systems produce coherent light with two orthogonally LP frequencies with frequency differences Δf between $1.5\,\mathrm{MHz}$ and $7.2\,\mathrm{MHz}$.
- The frequency stability measured over one hour of all their systems is $\pm 2\,\mathrm{ppb}$.

3.3 Zygo Corporation

Another a well known manufacturer of interferometric systems is Zygo. They use the comparison of axial modes method to stabilize a He-Ne laser tube and then use an AOM [39], [29]. This approach produces a difference frequency much lower than usually produced with the comparison of axial modes method. This has the advantage of easier signal processing in the heterodyne MI. The features of their systems are.

- The output power off all their systems is $\geq 0.4\,\mathrm{mW}$.
- Their systems produce coherent light with two orthogonally LP frequencies with a frequency difference of $\Delta f = 20\,\mathrm{MHz}$.
- The frequency stability measured over one hour of their most stable system is $\pm 0.5\,\mathrm{ppb}$.

3.4 Summary

Company	Output power	Δf	Frequency stability
Sios	$\geq 0.8\,\mathrm{mW}$	-	$\pm 2\,\mathrm{ppb}$
Agilent	$\geq 0.12\,\mathrm{mW}$	$7.2\,\mathrm{MHz}$	$\pm 2\,\mathrm{ppb}$
Zygo	$\geq 0.4\,\mathrm{mW}$	$20\,\mathrm{MHz}$	$\pm 0.5\,\mathrm{ppb}$

Table 3.1: The properties of the stabilized He-Ne laser sources with the highest frequency stability of the introduced companies.

In this chapter we describe some commercial available stabilized He-Ne laser sources from three different companies.
Table 3.1 summarizes the products with the highest frequency stability. It is evident that all products have almost the same stability. Only the product from Zygo has a higher stability. Since Zygo uses the comparison of axial modes methods, we are assured in our choice (section 2.2.4) of the comparison axial mode method.

4 Thermal Stabilization of a He-Ne Laser Tube

In section 2.1 we show that the frequency variation of coherent light depends on the frequency variation of the axial modes. Furthermore, in section 2.2 we discuss the most prominent methods to stabilize a He-Ne laser tube so that it emits coherent light with two orthogonally LP frequencies. Thereby we compare this methods and list some of their advantages and disadvantages. Based on that knowledge we choose the comparison of axial mode method. This method provides very good performance and is easy to implement.

Before building a standalone stabilized He-Ne laser tube, we test the concept and the suitability of each available He-Ne laser tube. We determine whether, or not the polarization of each axial mode stays constant. We determine whether or not the waste beam is suitable for obtaining the control variable. And we examine the warmup behaviour of the available He-Ne laser tubes.

This chapter describes the assembly and its major components. Furthermore, it describes the experiments and finally it explains the selection of the control algorithm.

4.1 Experimental Assembly

This approach is based on the comparison of axial modes method. The only difference is that we now use the waste beam of the He-Ne laser tube to derive the control variable for the control algorithm. This has the advantage that the intensity of the output beam is not weakened. The stabilization of the length of the optical cavity is done by thermal feedback. This means that we control the length of the He-Ne laser tube and, therefore, the length of the optical cavity by heating the laser tube.

Figure 4.1 shows the schematic of the experimental assembly, which is placed on an optical table. For the thermal stabilization we wrap a heating wire around the He-Ne

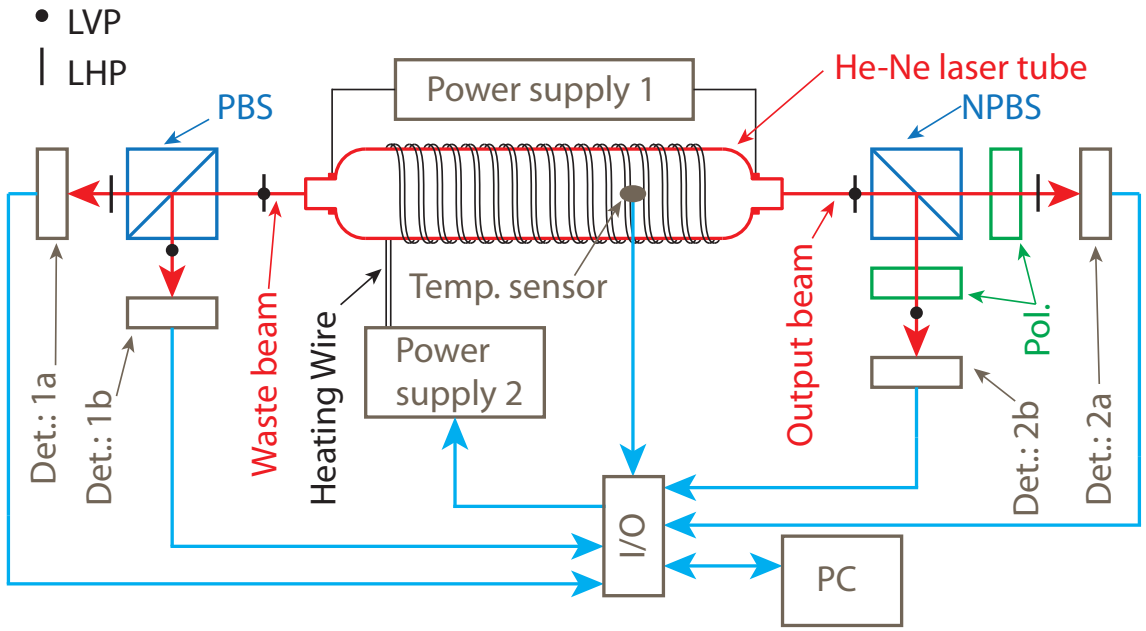

Figure 4.1: The experimental assembly of the comparison of axial modes methods. It consists of a He-Ne laser tube with a bifilar heating wire wrapped around it. The power supplies, of the laser tube and the heater, and the detector assemblies including the data acquisition. A PC is used to measure the data end execute the control algorithm.

laser tube. This heating wire has to be wrapped bifilar so that the resulting magnetic field from the heater is zero. Otherwise the created magnetic field causes a Zeeman-split of the gain curve, as described in section 2.2.2. The He-Ne laser tube is adjusted so that its axial modes are LHP and LVP. To monitor the temperature of the He-Ne laser tube we place six temperature sensors on its surface. The waste beam exiting the rear end of the He-Ne laser tube impinges on a PBS which splits the incident coherent light according to the polarization states of the axial modes. The resulting two beams are each directed to a detector, which produce electrical signals proportional to the intensity of the incident axial modes. We use a NPBS and two polarizers to measure the intensity of each axial mode in the output beam. The NPBS splits the output beam into two beams with nearly the same intensity and the two polarizers each block either the LVP or LHP axial mode so that the detectors only see the intensity of one axial mode.

The electrical signals produced by the detectors and the temperature sensors are all sampled using an Input/Output (I/O) module and further processed with a PC. Furthermore, the I/O module also holds besides the Analog Digital Converter (ADC), a Digital Analog Converter (DAC) by which we can control the voltage and consequently the current in the heating wire. Because the output power of the I/O module is too small to drive the

required current through the heating wire we use a programmable power supply to linearly amplify the output voltage of the I/O module.

The control variable for the thermal feedback is exclusively obtained by using the waste beam which exits the rear end of the He-Ne laser tube. The detection assembly on the front end of the He-Ne laser tube is only to compare the relation between the waste beam and the output beam.

4.1.1 Optical Components

In this section we describe the optical components which are used in the experimental assembly. We do not describe the NPBS and the polarizers, because they have no relevance for the thermal feedback control.

He-Ne laser tube
The light source in all experiments is a Siemens LGR-7641 He-Ne laser tube. The EMT possesses four of these tubes, which will be named LGR-7641-1 to LGR-7641-4. They have the following specifications.

- The intensity of the output beam is at least 0.65 mW.
- The intensity of the waste beam is at least 9.5 μW.
- The required power supply has to be capable to produce at least a voltage of 1 to 1.2 kV at a current of 3.5 mA.
- The tube is 243 mm in length and 30 mm in diameter.
- The length of the He-Ne laser tube is equivalent to the length of the optical cavity. Using equation 2.7 we can calculate that the frequency difference between the axial modes is approximately 616 MHz.
- Under the consideration that the FWHM of the gain curve of a He-Ne laser tube is approximately 1500 MHz, it is save to say that the emitted coherent light only consists of two axial modes.

Polarizing Beam splitter
The PBS with the model number 05BC16PC.4 [26] from Newport has the following specifications.

- The dimensions $H \times W \times L$ are 15 mm × 15 mm × 15 mm.
- The extinction ratio between the transmission of LHP light T_p and transmission of LVP light T_s is better than 1000 : 1.

- The transmission of LHP light with a wavelength of 632.8 nm is greater than 95 %.
- The reflection of LVP light with a wavelength of 632.8 nm is greater than 99.8 %.

4.1.2 Electrical Components

The following electrical components were used in this assembly.

Detectors 1
The detectors on the rear end of the He-Ne laser tube are high speed photo detectors DET36A [36] from Thorlabs with the following specifications.

- They produce an output voltage (V_{out}) between 0 to 10 V depending on the intensity of the incident light.
- The active area of the detector is 13 mm^2 (3.6 × 3.6 mm).
- The wavelength range is between 350 nm and 1100 nm.

Temperature sensor
The temperature sensors we use are the LM335 [25] from National semiconductor.

- The temperature range is from −55 °C to 150 °C.
- When calibrated at 25 °C it typically has less than 1 °C uncertainty over a 100 °C temperature range.

I/O module
We use the cDAQ-9172 [21] from National Instruments with the following three I/O modules.

- To sample the detector signals we use the NI 9215 [22] analog input module. It has 4 channels each with a maximum sample rate of 100 kS/s, 16 bit resolution, and an input range of ±10 V.
- To sample the temperature sensors we use the NI 9206 [24] analog input module. It has 16 channels with an overall sample rate of 250 kS/s, 16 bit resolution, and an input range of ±10 V.
- The analog output module is the NI 9263 [23] with 4 channels and 100 kS/s output rate. It has a resolution of 16 bit with a maximum output voltage of ±10 V.

Power supply 1
As power supply of our LGR-7641 He-Ne laser tube we use the power supply of a Melles Griot He-Ne laser tube. It's output voltage is between 1.85 and 2.45 kV with an output current at 6.5 mA.

Power supply 2
As power supply for the heating wire we use the Omega800 [18] power supply from Lambda with a programmable output voltage between 0 and 30 V.

Heating wire
We use 5 m of the RD 50/0.4 heating wire from Block for our bifilar heating coil. With a resistance of 3.9 Ω/m this leads to a overall resistance of 19.5 Ω. The heating wire was fixed by the means of a heat resistant duct tape.

4.2 Characteristics of the LGR-7641 He-Ne Laser Tubes

Before we implement a control algorithm for the thermal feedback using the comparison of axial mode method, we test each of the four LGR-7641 He-Ne laser tubes regarding their applicability for this method. Therefore, we investigate

- if the polarization state of each axial mode is constant,
- if the intensity of the waste beam is proportional to the intensity of the output beam, and
- the warmup behaviour of the He-Ne laser tubes.

This section describes the experiments, their results and solution approaches for any problems we find.

4.2.1 Polarizations Characteristics of the LGR-7641 He-Ne Laser Tubes

In the detection assembly on the rear end of the He-Ne laser tube the PBS splits the coherent light of the waste beam according to its polarization state. If the He-Ne laser tube is adjusted properly, i.e. so that the axial modes are LHP and LVP, each detector sees only the intensity of one axial mode. That is only when the polarization states remain

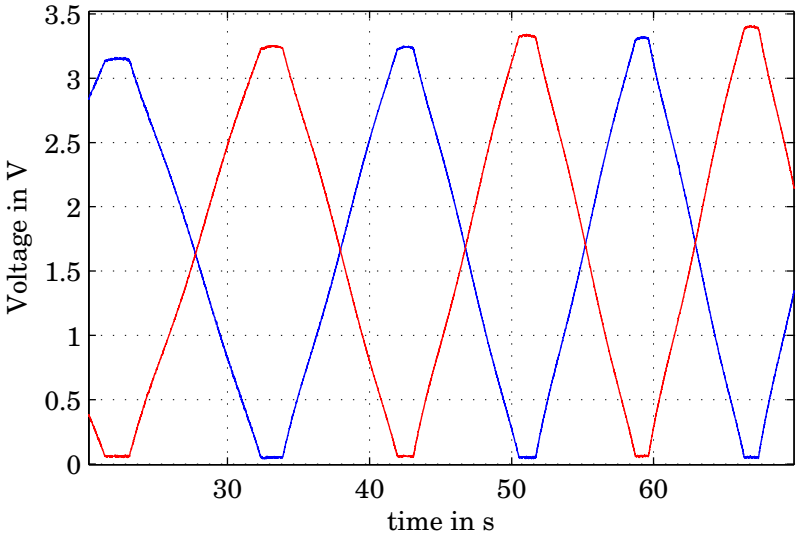

Figure 4.2: The mode sweep of the LGR-7641-1 between second 20 and 70 after activation. The red line shows the LHP and the blue line the LVP axial mode. It is evident that both polarization states remain constant.

constant. In case of changes in the polarization states the detector signals are no longer an indication for the true intensity of each axial mode. Such a case distorts the control variable for our future controller. The characteristics of the polarization states of the axial modes can be easily checked by looking at the so called mode sweep.

In a He-Ne laser tube the pumping mechanism producing the population inversion happens through electrical discharge in the gain medium. This process is not very efficient, so that typical He-Ne laser tube efficiency values are around 0.1%. Most of the dissipated power is converted into heat. After switching on the He-Ne laser tube, the emitted heat steadily rises until it converges to a constant value. This warmup is usually finished after a few hours. During this warm up phase the He-Ne laser tube experiences an expansion in length. According to equation 2.6,this leads to a decrease in the frequency of each axial mode. The axial modes, as depicted in figure 2.4, move to the left and change their intensity according to its position on the gain curve. If one axial mode moves under the laser threshold (equation 2.4), a new axial mode appears on the right hand side of the gain curve. The new axial mode has the same polarization state than the faded one. When we measure the intensities of the axial modes we see two periodic signals which frequencies depend on the length change of the He-Ne laser tube.

Figure 4.2 shows, a short part of the mode sweep measured at the waste beam of the LGR-7641-1 tube. Because the absolute values of intensities are of no concern we depict

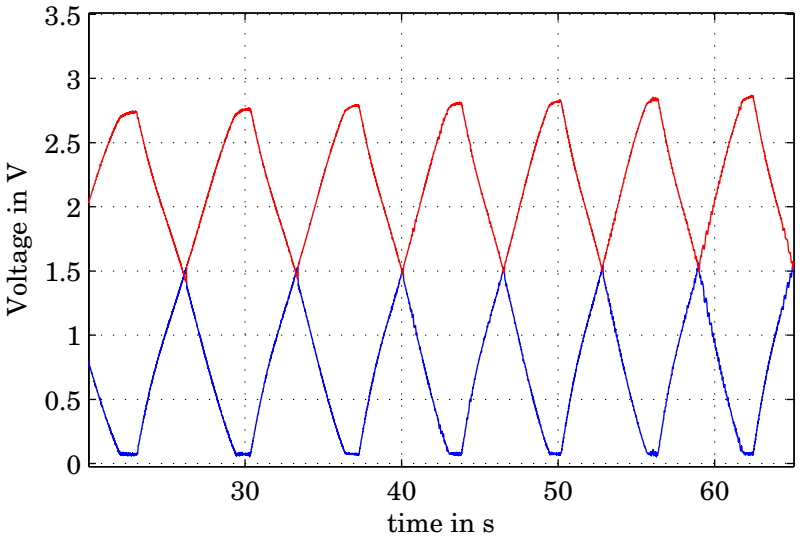

Figure 4.3: The mode sweep of the LGR-7641-4 between second 20 and 70 after activation. The red line shows the LHP and the blue line the LVP axial mode. It is evident that the polarization states switch shortly after both intensities are equal.

all measurements in voltage versus time. It is clearly evident that the intensity of each axial mode moves steadily from zero to maximum. This indicates that the polarization state of each axial mode remains constant. Tubes with such characteristics are very suitable for our stabilization scheme.

Figure 4.3, however, shows the mode sweep of the LGR-7641-4 tube. In this He-Ne laser tube the polarization states of the axial modes do not remain constant. It is clearly visible that, shortly after both intensities are equal, the polarization state of the axial modes switch. This makes the tube only marginally suitable for stabilization because the control variable, later used in our controller, is the difference between those two signals. A switch of the polarizations states results in the change of the sign of the control variable, thus leading to a decrease in the control performance. In more severe cases like when the polarization states switch when the intensities are closer their maximum respectively minimum, the controller could fail to reach steady state.

Because this effect origins in the properties of the optical cavity [13] and [29], there is no way to remove this effect. Luckily only one of our He-Ne laser tubes (LGR-7641-4) has this property, the others all have constant polarization states of their axial modes.

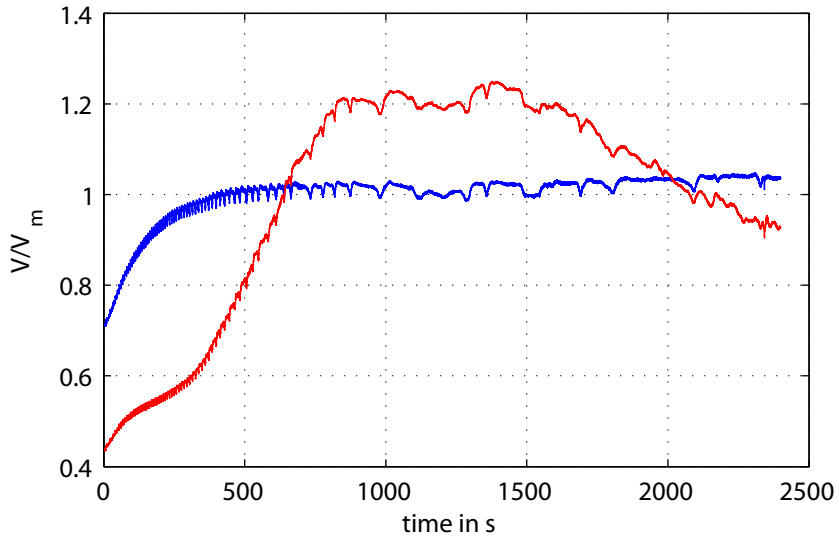

Figure 4.4: The intensity of the waste beam (red) and the output beam (blue) of the LGR-7641-1 He-Ne laser tube over a measurement period of 40 min, scaled by their mean values. The intensity behaviour of the waste beam is not proportional to the intensity behaviour of the output beam.

4.2.2 Comparison Between the Waste and Output Beam of the LGR-7641 He-Ne Laser Tubes

In our next experiment we check if the intensity characteristics of the waste beam, is proportional to the intensity characteristics of the output beam. This experiment is necessary because we do not use the output beam itself to generate the control variable, rather the waste beam. Our controller reacts according to the intensity changes in the waste beam. Any not proportional behaviour between waste beam and output beam leads to a decrease in the control performance.

To check if the intensity characteristic of waste beam and output beam is proportional to each other, we remove the PBS on the rear end of the laser tube. And we remove the NPBS and the polarizer on the front end of the tube. Thus allowing us to compare the changes in the overall intensities. Again we are only interested in the ratio between the two intensities and not in absolute values.

Figure 4.4 shows the intensity proportional voltage signals of the waste beam (red) and the output beam (blue) scaled by their mean value, versus time. It is evident that the intensity of the waste beam is not proportional to the intensity of the output beam. Unfortunately all of our He-Ne laser tubes show this characteristic.

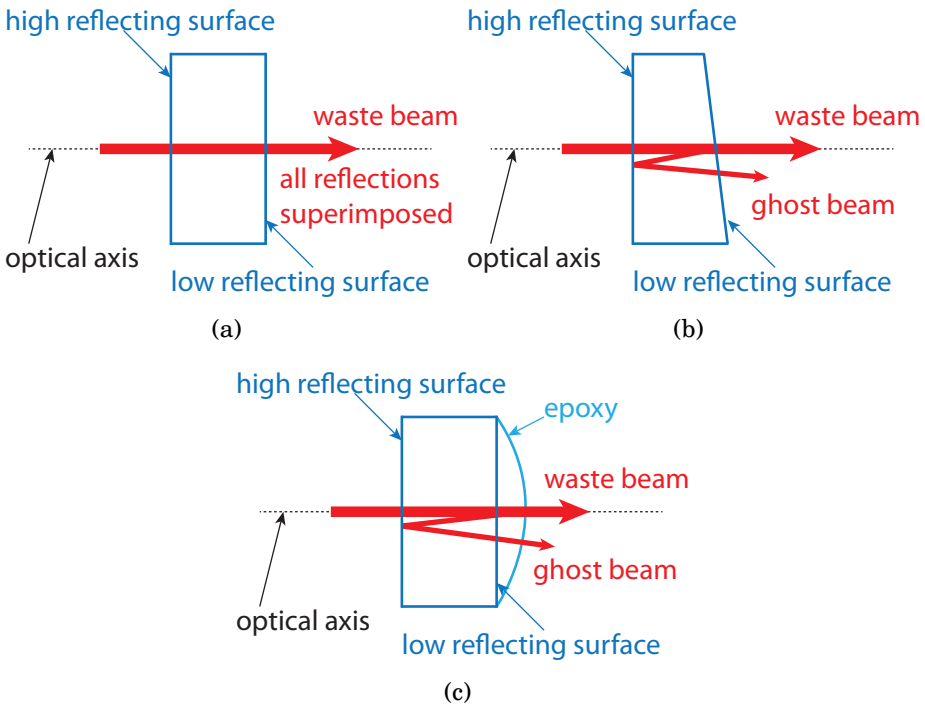

Figure 4.5: Three different types of HR mirrors of aHe-Ne laser tube. A HR mirror with parallel outer surfaces (a). A wedged HR mirror (b). A HR mirror with parallel outer surfaces and epoxy on its outer surface to improve the intensity characteristic of the waste beam (c). (Similar to [29].)

The reason for this behaviour lies in the construction of the HR mirror on the rear end of the He-Ne laser tube. The reflectivity of the inner surface of the HR mirror is not exactly 100 %. This allows the He-Ne laser tube to emit the waste beam. But the outer surface of the HR mirror also has a very low reflectivity. Which causes some reflection of the waste beam at the outer surface back into the optical cavity.

In our LGR-7641 He-Ne laser tubes the outer and inner surface of the HR mirror are parallel to each other and both orthogonal to the optical axis (figure 4.5(a)). The reflections from the outer surface, of the HR mirror are, therefore, all superimposed to the waste beam. This forms a second optical cavity between the outer and inner surface of the HR mirror. The transmission of the second optical cavity, depends on the frequency of the waste beam and the thickness of the HR mirror. Both are subject to variations due to the warm up. This second optical cavity is, therefore, responsible for the modulation of the effective reflectivity of the HR mirror and furthermore for the intensity variation in the waste beam [29].
Higher quality He-Ne laser tubes have a slightly wedged HR mirror. Such a mirror is

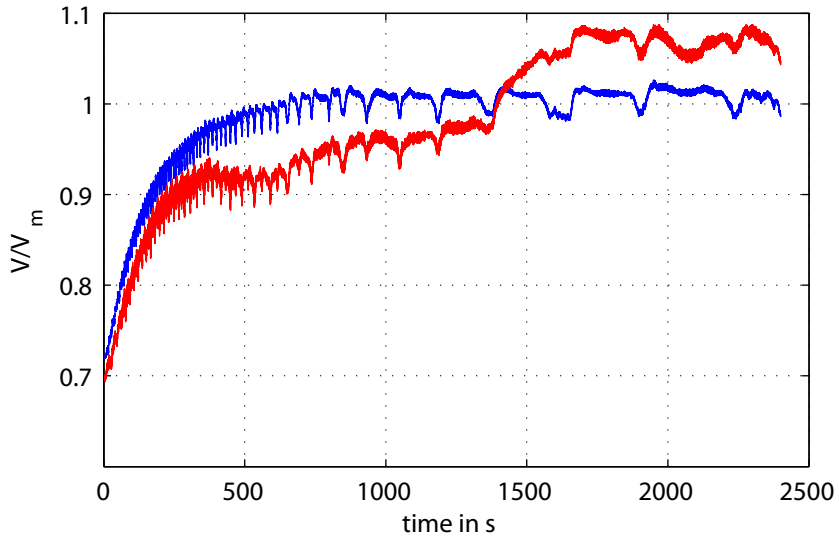

Figure 4.6: The intensity of the waste beam (red) and the output beam (blue) of the LGR-7641-1 He-Ne laser tube over a measurement period of 40 min, scaled by their mean values. The He-Ne laser tube was modified with a drop of epoxy on the outer surface of its HR mirror. Compared to figure 4.4, the characteristic of the waste beam has improved.

schematically depicted in figure 4.5(b). Note that the angle of the outer surface is in fact much smaller but, for better visualization, the angle is exaggerated. This wedge causes the reflection, from the outer surface, to be slightly off the optical axis. With no reflections along the optical axis no second optical cavity can build up which can modulate the reflectivity of the HR mirror. He-Ne laser tubes with wedged HR mirrors do not suffer from intensity changes of the waste beam. The beam reflected on the outer surface is reflected once more on the inner surface thus creating a ghost beam. This ghost beam is slightly off axis to the waste beam and, therefore, has no further relevance.
Figure 4.5(c) shows one solution [29] to modify the HR mirror so that it has almost the same properties as a wedged mirror. For this purpose we put a small drop of epoxy on the outer surface of the HR mirror. The epoxy almost has the same refractive index as the HR mirror, therefore, the reflection no longer occurs on the low reflecting surface rather on the surface of the epoxy. The resultant reflection is also slightly off the optical axis and, therefore, no direct reflections occur.

We modify the LGR-7641-1 He-Ne laser tube according to this solution and repeat the previous experiment. The result is shown in figure 4.6. Again it plots the waste beam (red) and the output beam (blue) scaled by their mean values, versus the time. It is evident that the intensity characteristic of the waste beam has improved. Although the behaviour between waste beam and output beam is still not perfect, it is an improvement

to the unmodified He-Ne laser tube. Apart from the intensity characteristic of the waste beam the drop of epoxy has some other effects on the He-Ne laser tube.

- The waste beam is now slightly off the optical axis. This must be taken into account when we adjust the PBS and the detectors.
- The waste beam is widened. This has absolutely no effect for the detection.
- The output beam has now a ghost beam. This is also not relevant because the ghost beam is slightly of axis and it is easy to prevent its interaction with any further application.

4.2.3 Warmup Behaviour of the LGR-7641 He-Ne Laser Tubes

As stated before the frequency variation of the emitted coherent light is in relation to the length of the optical cavity and this depends on

- the temperature changes of the ambient air,
- temperature changes of the He-Ne laser tube itself,
- pressure changes of the ambient air, and
- mechanical vibrations.

As stabilization method we select thermal feedback utilizing the comparison of axial modes. We use again the experimental assembly depicted in figure 4.1. The only modification is a perspex housing which we place over the He-Ne laser tube. This housing has holes to allow the two emitted beams to exit and one hole to allow wires to enter. The purpose of the housing is to shield the He-Ne laser tube from fluctuations of temperature and pressure of the ambient air. And it also serves as protection from the high voltage powering the He-Ne laser tube. Mechanical vibrations if present can be avoided by placing the He-Ne laser tube on an air suspended optical table. Thus leaving as main source for the length variations, the variations of the temperature of the He-Ne laser tube itself. In these experiments we focus on the temperature behaviour of our LGR-7641 He-Ne laser tubes.

Figure 4.7 shows the warmup of the LGR-7641-1 He-Ne laser tube over a period of five hours. Figure 4.7(a) shows the mode sweep measured on the waste beam. Red is the LHP and blue is the LVP axial mode. Figure 4.7(b) shows the difference between the two axial modes and, therefore, the future control variable. Figure 4.7(c) shows the temperature of the He-Ne laser tube. These three plots depict the relationship between the temperature, the axial modes, and the future control variable.

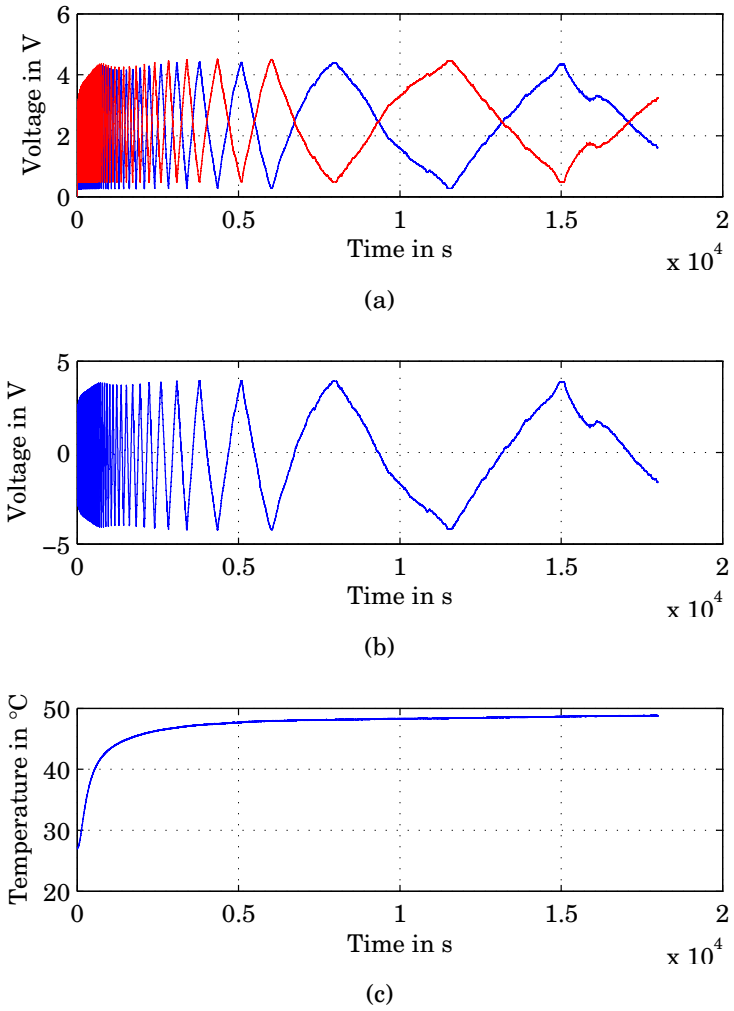

Figure 4.7: The warmup behaviour of the LGR-7641-1 He-Ne laser tube over a period of five hours. The mode sweep measured on the waste beam, red is the LHP and blue is the LVP axial mode (a). The difference between the LHP and LVP axial mode (b). The temperature of the He-Ne laser tube (c).

It is evident that the time response of the temperature corresponds to a PT-1 element. After one hour of operation the temperature reaches almost steady state.
The intensity of each axial mode is defined by its position on the gain curve figure 2.4. Their position on the gain curve, however, is in direct relation to the length of the optical cavity (equation 2.6). Since temperature changes influence the length of the optical cavity it is evident that the intensity of each axial mode is a function of the temperature change. In addition to that the experiments show that the operating temperature of the LGR-7641 He-Ne laser tubes is around 50 °C.

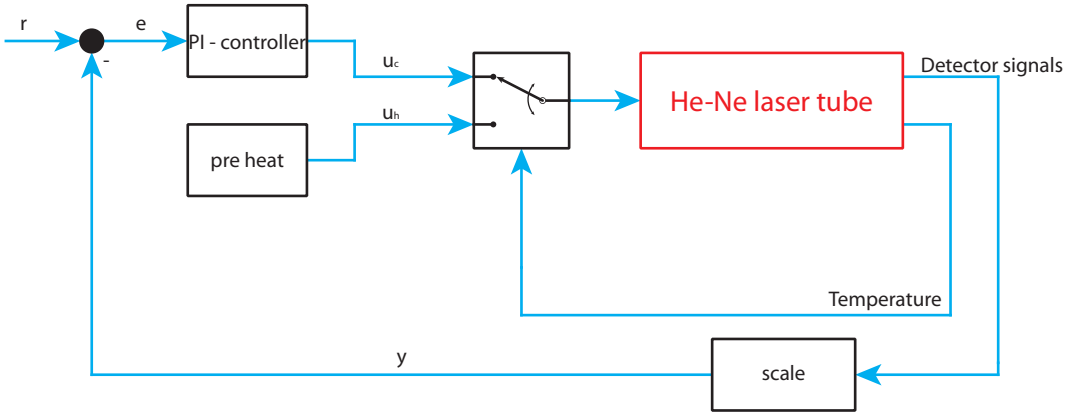

Figure 4.8: Block diagram of the implemented control algorithm. The two detector signals from the waste beam are scaled and subtracted, forming y. After we pre heat the He-Ne laser tube we activate a PI controller to thermally stabilize its length.

4.3 Control Algorithm

Based on the experimental assembly depicted in figure 4.1 we implement a control algorithm to stabilize the He-Ne laser tube using the comparison of axial modes method.

Figure 4.8 shows the block diagram of the implemented control algorithm. The two detector signals, representing the intensity of the LHP and LVP axial mode, are scaled and subtracted. This creates the control variable y. By applying a constant voltage u_h to the heating wire it is possible to pre heat the He-Ne laser tube above its usual operating temperature of 50 °C. When the temperature of the He-Ne laser tube has reached a certain point we activate the Proportional Integral (PI) controller. This controller calculates depending on the reference variable r and the control variable y the manipulated variable u_c which we apply to the heating wire.

Subsequent we describe starting with the PI controller the pre heat process and the need for scaling the detector signals before creating y.

4.3.1 PI Controller

In section 4.2.3 we state that the time response of the temperature corresponds to a PT-1 element. Therefore, we chose a PI controller to thermally stabilize the He-Ne laser tube. The controller works with a control frequency of 10 Hz. Due to the fact that the mode sweep has a maximum frequency of 0.2 Hz and because temperature changes usually are slow processes we thereby, implement a quasi continuous controller.

We tune the PI controller using the Ziegler-Nichols method [16]. The obtained results are not entirely satisfactory. Therefore, we manually tune the controller, to improve its time response and minimize the control deviation.
Because our controller has an integral part and a restricted manipulated variable, we require an anti-windup strategy. This anti-windup strategy is implemented by deactivating the integral part of the controller when its manipulated variable is above its upper or under its lower limit.
To balance both axial modes we have to set the reverence variable $r = 0$. A change in the reference variable, however, leads to a change in the temperature and, therefore, length of the He-Ne laser tube. This leads according to equation 2.6 and figure 2.4 to a change of the frequency and intensity of each axial mode.

4.3.2 Preheating of the He-Ne Laser Tube

Our PI controller reacts on positive control deviations with an increase in u_c and, therefore, to an increase in temperature which causes an expansion of the He-Ne laser tube. In case of negative control deviations the controller has to have the capability to decrease the temperature and, therefore, the length of the He-Ne laser tube. For this reason we decide to operate the He-Ne laser tube above its usual operating temperature of 50 °C. This allows the controller to cool down the He-Ne laser tube and to react on a negative control deviations as well.
We preheat the He-Ne laser tube with a constant voltage until the temperature rise and the frequency of the mode sweep is low and then activate the controller. This temperature is around 60 °C.

4.3.3 Scaling of the Detector Signals

If the detectors on the waste beam are not aligned properly it is possible that the ratio between the intensities of the two axial modes is distorted. Similarly, the occurrence of residual light can produce an offset in the intensity measurement. Both leads to a distortion of the controlled variable. Note that the intensities of the output beam remains undistorted.
Our stabilization method is based on the comparison of the intensities of the axial modes and our PI controller is optimized for a control variable ranging from -4 to $+4$ V. Therefore,

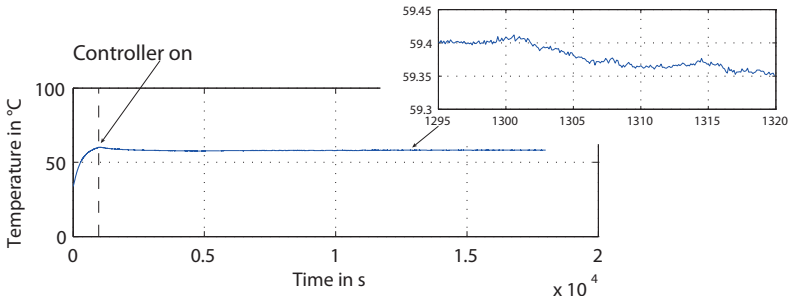

(a)

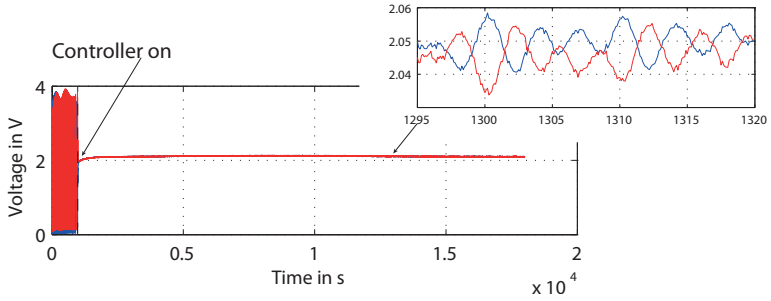

(b)

Figure 4.9: The behaviour of the control algorithm over a period of 5 hours. The temperature behaviour (a). The detector signals, red is the LHP and blue is the LVP axial mode (b).

we decide to scale the detector signals using

$$det_{x,scaled} = (det_x - min(det_x)) \frac{4}{max(det_x) - min(det_x)}, \tag{4.1}$$

where det_x is the current intensity value of either the LHP or LVP axial mode, $min(det_x)$ and $max(det_x)$ are the scaling parameters, and $det_{x,scaled}$ is the scaled intensity value. We use the first few seconds of the mode sweep during the pre heat phase to acquire the scaling parameters. Note that the scaling can only compensate for misalignment in the detectors and not for the misalignment of the He-Ne laser tube.

4.3.4 Behaviour of the Control Algorithm

Figure 4.9 and figure 4.10 show the behaviour of the control algorithm over 5 hours. We see the temperature (figure 4.9(a)), the scaled detector signals of the axial modes measured on the waste beam (figure 4.9(b)), the control variable (figure 4.10(a)), and the manipulated variable (figure 4.10(b)).

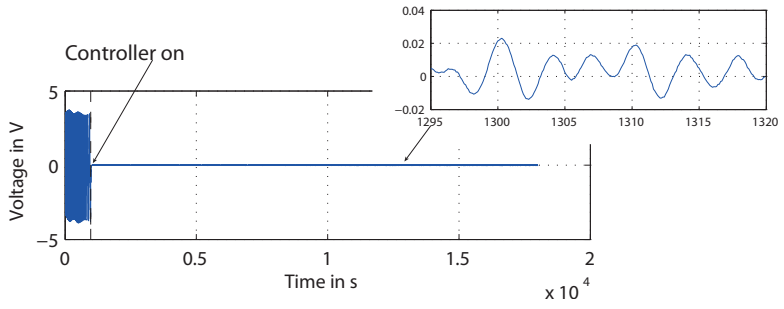

(a)

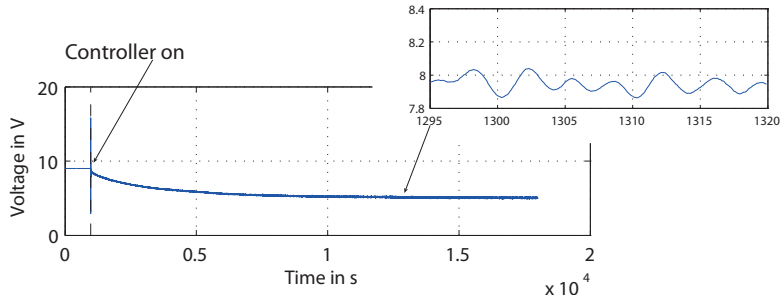

(b)

Figure 4.10: The control variable (a). The manipulated variable (b). After approximately 15 minutes we activate the controller. Before activating the PI controller we preheat the He-Ne laser tube to 60 °C. This takes around 15 minutes. The control variable follows the reference variable. It takes around 2 hours to reach thermal equilibrium.

By applying a constant voltage of 9 V to the heating wire we pre heat the He-Ne laser tube to approximately 60 °C and activate the controller. The pre heat process takes approximately 15 minutes.
After the activation of the controller the control variable follows the reference variable which is set to zero. In all our experiments the control deviation never exceeds an error band of $\epsilon = \pm 0.1$.
We can see that after the activation of the controller the He-Ne laser tube is still not in the thermal equilibrium. It takes around 2 hours for the system to reach thermal equilibrium.

4.4 Summary

In this chapter we describe the results of the experiments which we make in order to prepare for the implementation of our stabilization scheme in hardware. We describe

the experimental assembly, with its optical and electrical components. We show two experiments in which we examine the polarizations characteristics of the axial modes and the intensity characteristic of the waste beam. We find that one of our LGR-7641 He-Ne laser tubes is not suitable for our stabilization scheme and that all our LGR-7641 He-Ne laser tubes have a non proportional behaviour regarding the waste and the output beam. We solve the problem by putting a drop of epoxy on the HR mirror, thus making the He-Ne laser tube suitable for our stabilization scheme. We depict the warmup behaviour of the LGR-7641 He-Ne laser tubes and conclude that we have to preheat the He-Ne laser tube before we can activate the controller. We implement a PI controller and show the behaviour of our control algorithm.

5 Construction of a Standalone Stabilized He-Ne Laser Source

This chapter describes the construction of a standalone thermally stabilized He-Ne laser source. We design three circuit boards for the needed electronics, implement the control algorithm on a Microcontroller Unit (MCU) in C, and design a housing for all the required components. Therefore, this chapter is divided in three sections each deals with one of the three stages of construction.

5.1 Electrical Components of the Standalone Stabilized He-Ne Laser Source

To implement the control algorithm which we describe in section 4.3 the hardware must be able to

- measure the temperature of the He-Ne laser tube,
- measure the intensities of the axial modes in the waste beam,
- execute the control algorithm,
- and amplify the calculated manipulated variable in order to apply it to the heating wire.

To meet the requirements in section 1.2 the hardware also must be able to

- output the measured intensities of the axial modes,
- measure a voltage signal provided from an external controller,
- query a switch,
- and give an indication whether or not the frequency of the coherent light is stable. This is done by setting a status Light Emitting Diode (LED) and applying +5 V Direct Current (DC) to one of the Bayonet Neill Concelman (BNC) sockets.

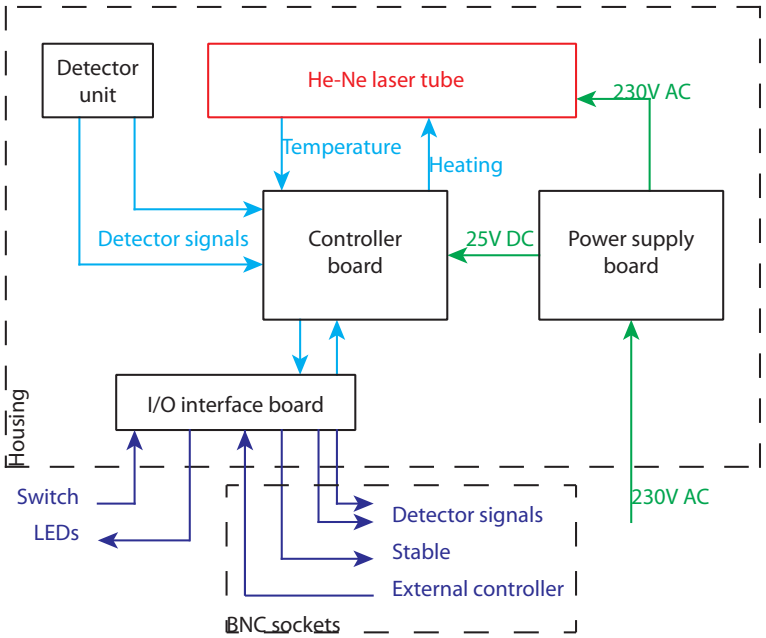

Figure 5.1: Basic overview of the designed hardware. The power supply board provides the 230 V AC for the power supply of the He-Ne laser tube and the +25 V DC for the controller board. The controller board executes the control algorithm. The I/O interface board connects the controller board to the BNC sockets, the LEDs, and the switch.

Figure 5.1 gives a basic overview of the hardware. The power supply board requires 230 V Alternating Current (AC) as input voltage. It supplies the controller board with +25V DC and the power supply of the He-Ne laser tube with 230 V AC.
The controller board measures the input signals, and executes the control algorithm.
The I/O interface board connects the controller board with the BNC sockets, the switch, and the status LEDs.

We use the same heating wire to heat the He-Ne laser tube and one LM335 temperature sensor to measure its temperature. Both components are described in section 4.1.2. Only modification is that we glue both to the surface of the He-Ne laser tube.
We measure the intensities of the axial modes in the waste beam with two Silicone PIN photo diodes BPX 65 from Osram [27]. The photo diodes are located on the detector unit (section 5.3.1). We use shielded cables to bring their signals to the controller board.

5.1.1 Power Supply Board

The hardware in the standalone stabilized He-Ne laser source requires three different voltages. The power supply of the He-Ne laser tube requires 230 V AC. The controller

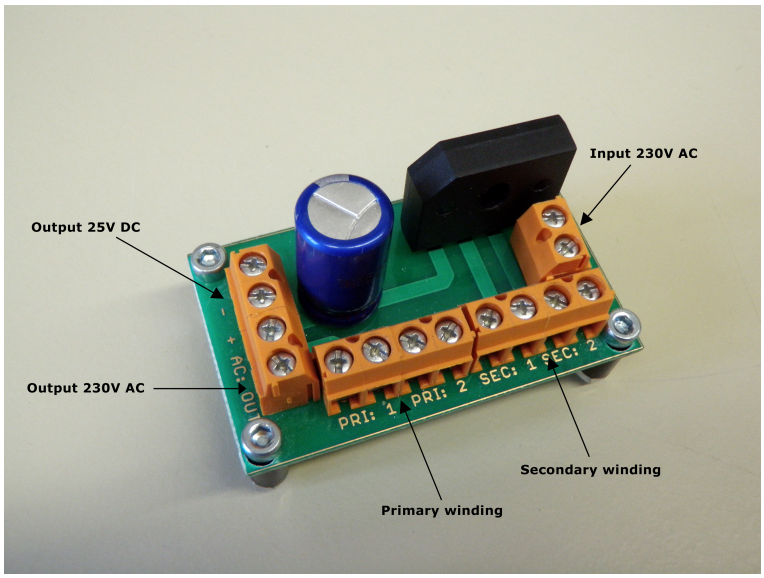

Figure 5.2: Besides the toroidal transformer and the bridge rectifier, the power supply board holds the connections for the input voltage, the output voltages, and the toroidal transformer.

board requires +5 V DC for the electronics and a DC high enough to provide sufficient power to the heating wire. As depicted in figure 4.10(b), the voltage applied to the heating wire never exceeds +16 V DC, which equals a heating power of 13 W.

Since we only want one power connection in our stabilized He-Ne laser source we need a power supply board (figure 5.2) to produce the required DC voltages. To decrease the development risk, we select a 40 VA/18 V toroidal transformer from Block and a bridge rectifier which produces a voltage of +25 V DC. This voltage is suffice to provide the necessary heating power.
The toroidal transformer has two primary windings each with a nominal input voltage of 115 V AC, we need to couple those two windings in series in order to input 230 V AC. We also connect the secondary windings in parallel to double the secondary nominal current.

5.1.2 Controller Board

To execute the control algorithm we build a controller board, depicted in figure 5.3. We choose the ATMEGA32 [2] MCU with an external 16 MHz oscillator. This MCU has all the required features, like an eight channel 10-bit ADC, two timers capable of creating a Pulse Width Modulation (PWM) signal and sufficient I/O ports.

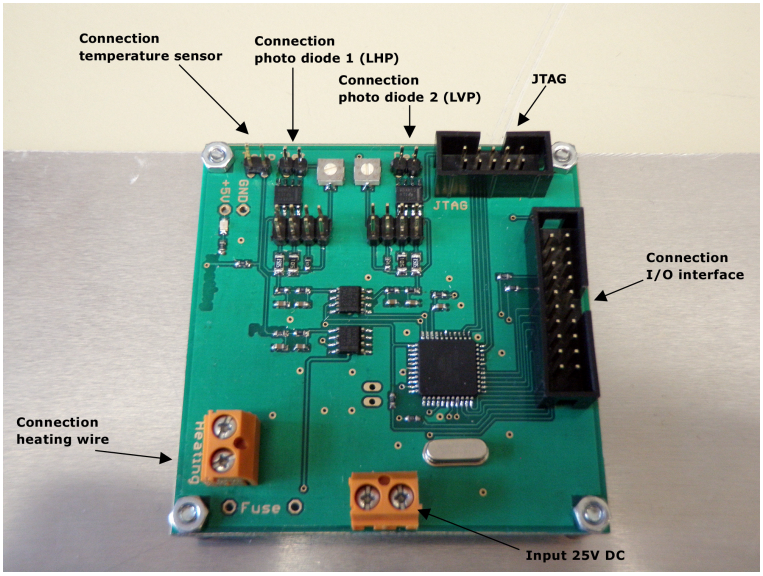

Figure 5.3: The controller board holds the MCU and all its required periphery to execute the control algorithm. It also holds connections to the photo diodes, the temperature sensor, the heating wire, the I/O interface board, and the Joint Test Action Group (JTAG) interface.

The MCU outputs the manipulated variable via a PWM signal. We amplify this signal using the +25V DC input voltage and a N-channel Metal Oxide Semiconductor Field Effect Transistor (MOSFET). We use a linear voltage regulator to generate the required +5V DC for the electronics. Because the linear voltage regulator converts its power loss into heat we placed it on the bottom layer to dissipate the heat over the future housing.

Figure 5.4 shows the input circuitry of the controller board. The amplifying circuit of the photo diodes consists of a Current to Voltage (C/V) converter, using the OPA140 from Texas Instruments. We can adjust the gain of the C/V converter by increasing or decreasing the feedback resistance. This provides a first compensation for a possible misalignment of the photo diodes. We apply the signals to a Anti aliasing filter (AAF). The filtered signal now goes through an impedance converter and is then applied to the ADC of the MCU and to the I/O interface board.
The input circuit of the temperature signal is identical to the input circuit of the detector signals, only that the C/V converter is replaced with the connection of the temperature sensor.
The analog input voltage of an external controller is applied to a first order AAF and is then applied to the ADC. For protection from voltages higher than ±5V, the MCU possesses internal clamp diodes. Since the maximum permissible current through the clamp diodes is ±1mA, the lowpass filter also acts as a current limiter. The MCU is,

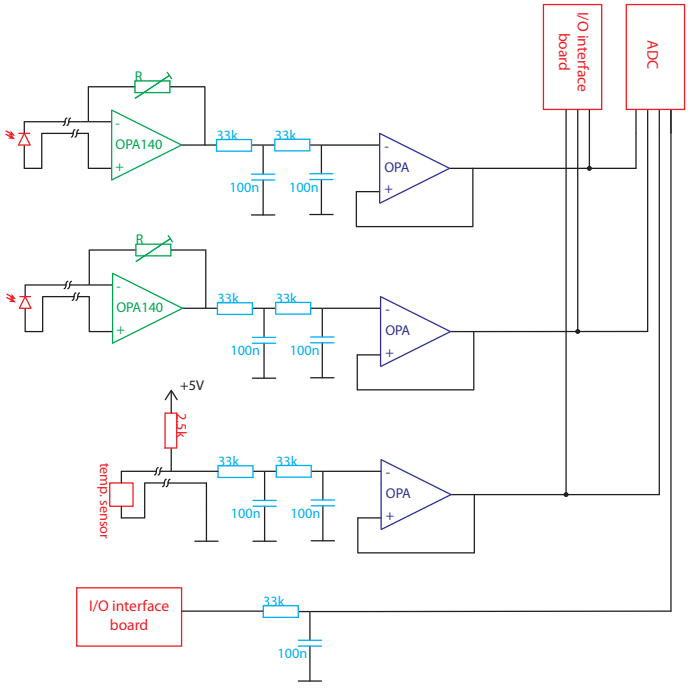

Figure 5.4: The input circuit on the controller board to measure the intensity of the axial modes, the temperature of the He-Ne laser tube, and a voltage signal provided from an external controller.

therefore, protected against voltages up to ±10 V.

We choose a sample frequency of 1 kHz. This is done to keep the design of the AAFs simple. We choose the AAFs to be second order lowpass filters with a cutoff frequency of $f_c = 48\,\text{Hz}$. Only the AAF of the external controller is a first order low pass filter ($f_c = 48\,\text{Hz}$). This is done because the Data sheet of the ATMEGA32 recommends a low source impedance for its ADC [2].

5.2 Software of the Standalone Stabilized He-Ne Laser Source

This section describes the program that was written to implement the control algorithm on the ATMEGA32 MCU. We implement the software in C using the AVR Studio™5 from ATMEL. The program

- sets the sample frequency of the ADC to 1 kHz,
- digitally filters the input signals using a 20-point moving average filter,

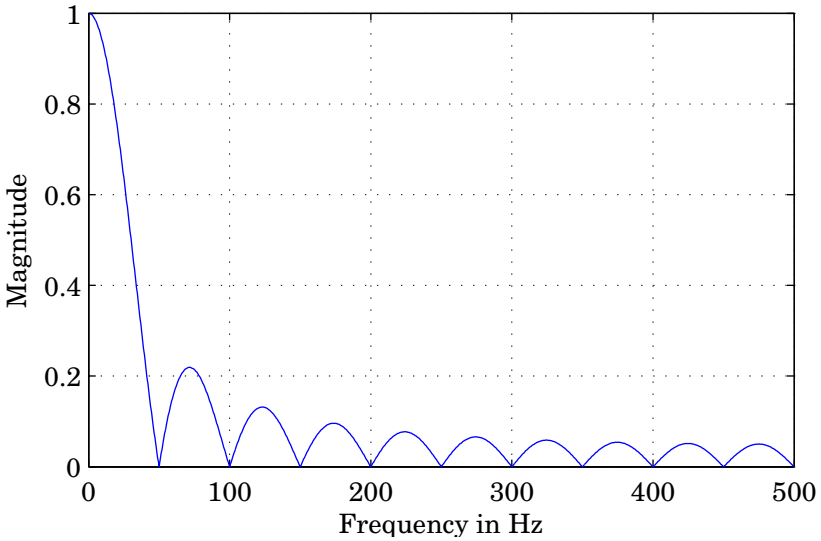

Figure 5.5: The frequency response of a 20-point moving average filter. Integer multiples of the frequency 50 Hz are completely eliminated by the filter.

- and calls the control algorithm every 100 ms.

Starting from the controller parameters which we obtain in the experiments described in section 4.3, we manually tune the PI controller to optimize its performance.
The PI controller works with a frequency of 10 Hz and it is calculated in float. The manipulated variable is output via a 8-bit PWM signal with a frequency of 62.5 kHz. This frequency is determined by the clock frequency of the MCU and the used 8-bit timer. We determine the operating temperature of the standalone He-Ne laser tube by applying a constant voltage to the heating wire and look at the mode sweep. We find a new operating temperature of 80 °C.
To further reduce noise in the input signals caused by the mains frequency we use a moving average filter to filter the input signals. Figure 5.5 shows the frequency response of a 20-point moving average filter. We choose its length so that integer multiples of the mains frequency (50 Hz) are completely eliminated.

In the following two sections we describe the data acquisition and the implemented control algorithm.

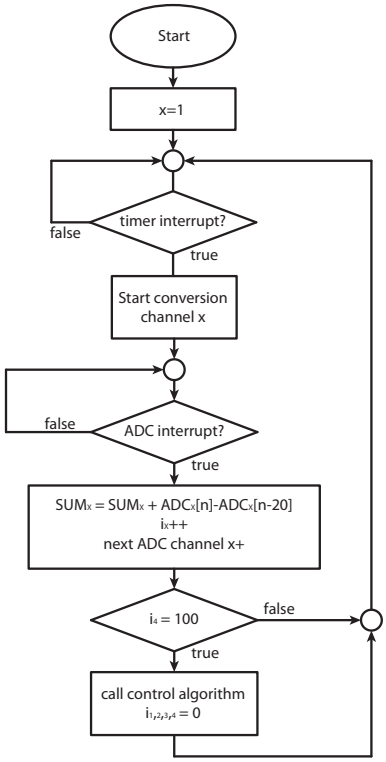

Figure 5.6: The flowchart of the implemented data acquisition. The timer interrupt is called every 250 μs. The ADC conversion is finished after 52 μs. This approach ensures a constant sampling frequency of 1 kHz.

5.2.1 Data Acquisition

Figure 5.6 shows the basic flowchart of the data acquisition. We set one 8-bit timer to trigger a hardware interrupt every 250 μs. This hardware interrupt orders the ADC to start a single conversion of the voltage applied to the first ADC channel $x = 1$. The ADC clock runs with a frequency of 250 kHz. Since one ADC conversion requires 13 ADC clock cycles, it takes around 52 μs to finish one conversion. After one conversion is finished the ADC triggers an ADC interrupt. In which we compute the ADC value with the given equation

$$SUM_X = SUM_X + ADC_X[n] - ADC_X[n-20], \tag{5.1}$$

where SUM_X is the sum of the ADC values of the channel x, $ADC_X[n]$ is the current ADC value, and $ADC_X[n-20]$ is the ADC value acquired 20 conversions ago. We also increase a counter variable for the channel i_x++ and we set the ADC to the next channel $x+$. Note that when the channel $x = 4$ the interrupt sets the channel to $x = 1$.
When the counter variable i_4 has reached 100, this happens every 100 ms, we reset the

counter variable $i_{1,2,3,4} = 0$ and call the control algorithm.

At the beginning of every cycle of the control algorithm we divide the acquired sum of the ADC values SUM_X by the value 20. This digitally filters the input signals by a 20-point moving average filter. Note that while the control algorithm is executed the data acquisition as depicted in figure 5.6 continues.
This approach ensures that every input signal is sampled at a constant frequency of 1 kHz. And it ensures that the control algorithm and, therefore, the PI controller works with a frequency of 10 Hz.

5.2.2 Overview of the Control Algorithm

Figure 5.7 shows the basic flowchart of one cycle of the control algorithm as it is performed every 100 ms.
The first task in every control cycle is to divide the input signals by 20. This is the final step in the data acquisition and is necessary for the computation of the 20-point moving average filter. The function converts the input signals representing the intensity of the LHP and LVP axial mode into float variable. The temperature signals and the signal from the external controller remain as integer variables because we do not need them for any computation.
Since the operating temperature is at 80 °C we imply that at a temperature above 120 °C, either the external controller or the implemented PI controller malfunctions. To prevent senseless heating of the He-Ne laser tube we implement the *overheat* function. This function sets the PWM signal to zero until the temperature has reached a temperature of 55 °C. We choose the value of 120 °C arbitrarily because we do not want to limit the operating temperature of any future external controller.
Next the control algorithm checks if scaling variables are present or not. In case no scaling variables are available, the control algorithm calls the *acquire scale* function. Once called this function is called the next 200 times, which equals 20 seconds. This function sets the PWM signal to a high value in order to heat the He-Ne laser tube and to force a fast mode sweep. The fast mode sweep is used to detect the scaling parameters for the signals representing the LVP and LHP axial modes. Once it has acquired these variables the function is never called again. If the scaling variables are available the function *scale signals* will scale both signals using the equation 4.1.
If at least one of the two scaling parameters which represent the maximum value of the intensities of the axial mode is below 1 we call the *safety function*. This function sets the PWM signal to zero and prohibits any further heating of the He-Ne laser tube. This

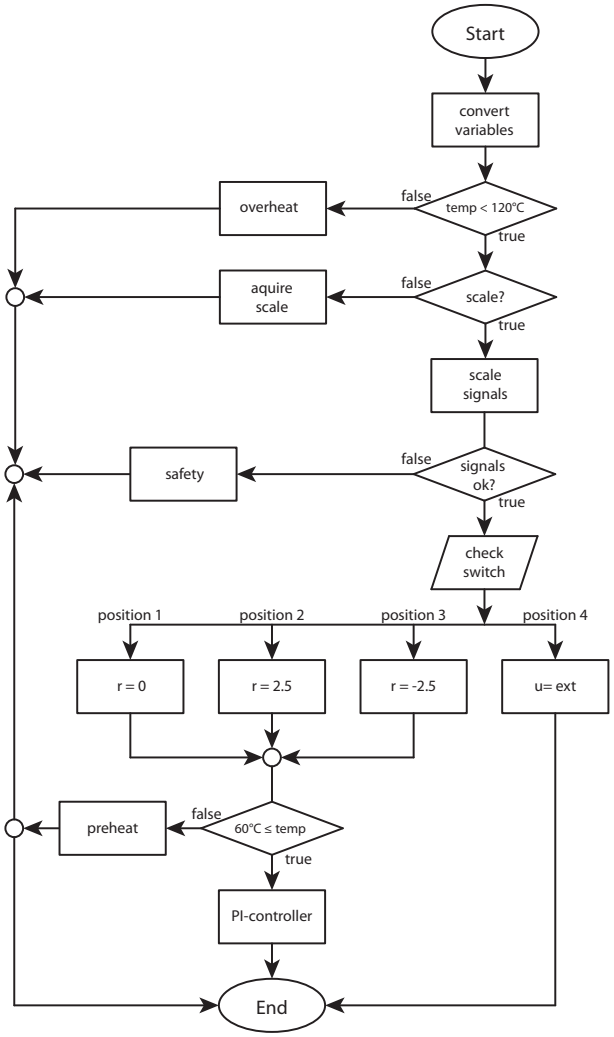

Figure 5.7: The basic flowchart of the implemented control algorithm, as it is performed every 100 ms, with all its important functions and instructions.

shall prevent from improper alignment of the He-Ne laser tube or any failure in the input circuit. The value of 1 is arbitrarily chosen.
The next step in the control algorithm is to check the rotary switch for its position. The first three positions set the reference variable to a certain value, which allows the PI controller to either balance the intensities of the axial modes or to increase the intensity of one of the two.
But before it can do so, the control algorithm finally checks the temperature and if its value is below 60 °C it calls the *preheat function*. This function sets the PWM so that it slowly heats the He-Ne laser tube to a temperature of 80 °C. We implement this lower boundary for the operating temperature because the temperature tends to drift

figure 4.9(a). This drift can be increased by changing the reference variable or switch to the external controller and back. The value of 60 °C is chosen arbitrarily, since it is still above 50 °C. The controller also sets a status LED on the I/O interface when the control deviation is within an error band of $\epsilon \pm 0.1$. This indicates that the controller reached steady state.
The fourth position of the rotary switch tells the control algorithm to linearly apply the voltage from an external controller via the PWM to the heating wire. $0-5\,\mathrm{V}$ equals $0-100\,\%$ of the duty cycle of the PWM.

The reader is refereed to figure A.1 in the appendix. It summarizes the basic functions, the meaning of the LEDs and, the BNC sockets.

5.3 Mechanical Components of the Standalone Stabilized He-Ne Laser Source

The last section of the current chapter deals with the mechanical components of the stabilized He-Ne laser source. It is divided into two parts. The first part explains the detector unit which carries the PBS and the photo diodes. The second part explains describes the entire housing.

5.3.1 Detector unit

Figure 5.8 shows the detector unit which we use in this thesis. It was designed by Auer in the course of his master project [3]. It holds the PBS described in section 4.1.1, three apertures and two photo diodes where each is connected to a pin connector. If the detector unit is closed, it protects the photo diodes from residual light. Furthermore, it is possible to fix the detector unit using four M6 screws.

5.3.2 Housing of the Stabilized He-Ne Laser Source

Figure 5.9(a) and figure 5.9(b) show the constructed laser housing, which contains all necessary components like the He-Ne laser tube and its power supply, the 3 circuit boards, the toroidal transformer, and the detector unit.

The laser housing consists of a 8 mm aluminium baseplate and at its four edges we place four carriers. We use the carriers to attach the two side panels, the front panel, the rear

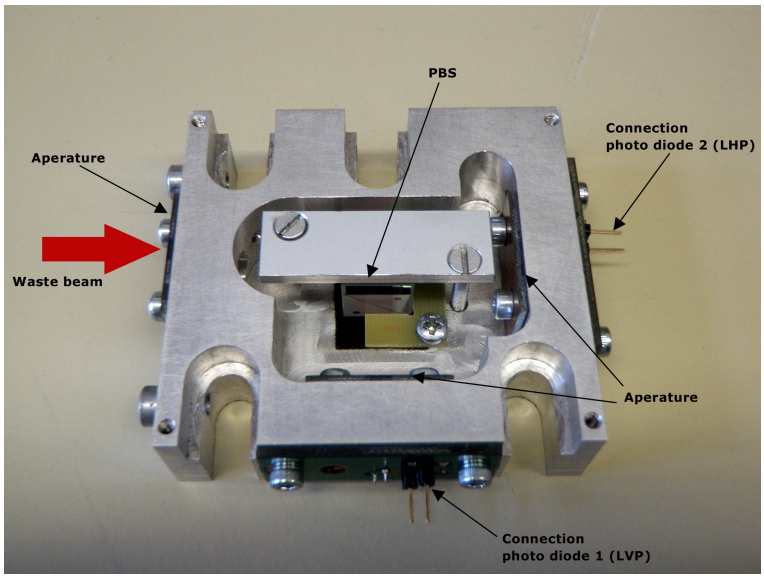

Figure 5.8: The opened detector unit with the mounted PBS. The coherent light from the waste beam enters through the aperture. The PBS splits the coherent light according to its polarization states and directs the light to the photo diodes. We use shielded cables to bring the signals from the photo diodes to the controller board [3].

panel, and the top panel. One side panel, the front panel, and rear panel are of 2 mm aluminium plates. The remaining side panel and the top panel are made of 5 mm perspex. The front panel has a hole to allow the coherent light from the He-Ne laser tube to exit the housing.
We attach the controller board and the power supply board to the aluminium side panel. The I/O interface board, however, is attached on the rear panel. The rear panel has holes to mount the four BNC connectors, the rotary switch and the four status LEDs.
To avoid displacements at the front end of the He-Ne laser tube and, therefore, displacements of the coherent light beam it is necessary to fix the front end of the He-Ne laser tube. Therefore, we directly attach the laser tube to the front mounting.
Since the He-Ne laser tube is subject to a thermal expansion it is necessary to allow a little movement of the rear end of the tube. Therefore, we attach an O ring between the laser tube and the rear mounting.
The detector unit rests upon two opposed aluminium corner plates. This allows us to change the height and the azimuth angle of the detector unit, in order to align it properly. Beneath the detector unit we attach the toroidal transformer to the baseplate.

The constructed housing is 400 mm in length, 140 mm in width and 133 mm in height. The coherent light exits at a height of 120 mm.

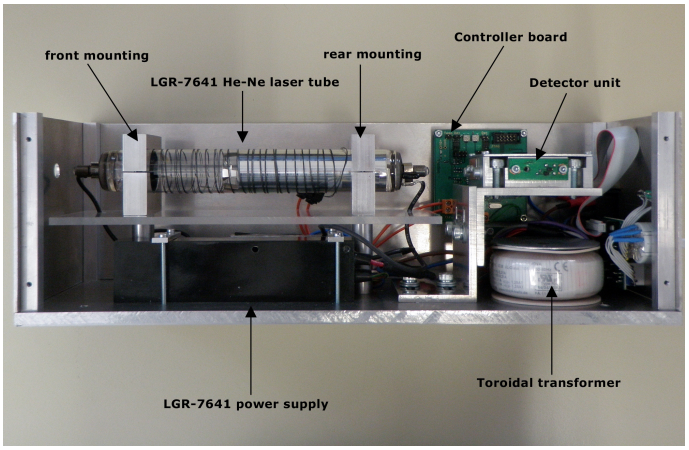

(a)

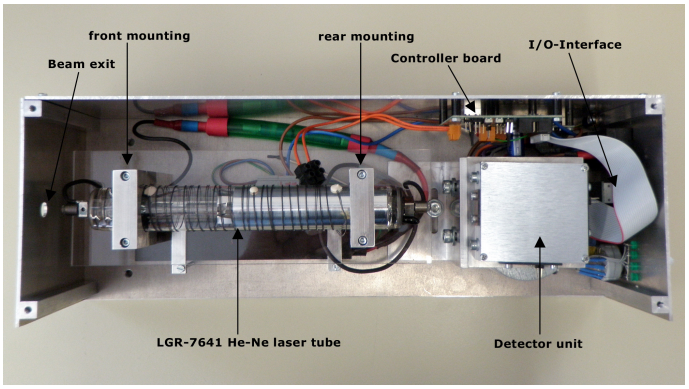

(b)

Figure 5.9: The profile (a) and the top view (b) of the standalone stabilized He-Ne laser source, with all its components. The top and one side plate is removed. The housing is designed to minimize its size.

5.4 Summary

Our stand alone stabilized He-Ne laser tube requires a 230 V AC supply voltage to operate. The electronics inside are capable of measuring the intensity of the axial modes in the waste beam, the temperature and an external voltage signal. It is capable of either stabilize the He-Ne laser tube using its internal PI controller or amplifying a input voltage from an external controller and apply it to the heating wire. The laser housing contains all required components and was made out of aluminium and perspex.

6 Experiments and Findings

This chapter describes the experiments which we make to characterize the performance of our standalone stabilized He-Ne laser source. We describe the measurement assembly and the experiments. Finally we state suggestions to improve the stability of our standalone stabilized He-Ne laser source and to improve the uncertainty of our measurement method.

6.1 Measurement Assembly

Figure 6.1 depicts the measurement assembly which is build to test the performance of our standalone stabilized He-Ne laser source. The single mode LP coherent light from the SL-03 He-Ne laser [33] goes through a polarization maintaining optical fiber and is decoupled with a fiber coupler. The NPBS splits the coherent light into two beams with approximately the same intensity. The transmitted beam is of no concern. The reflected beam, however, is coupled into a second polarization maintaining optical fiber. This optical fiber routes the coherent light to a high speed photo detector.
The dual mode coherent light of the stabilized He-Ne laser tube goes through a polarizer, which allows us to block one of the two axial modes, and hits the NPBS. The reflected part of the coherent light has no relevance. The transmitted part is also coupled into the second polarization maintaining fiber and goes to the detector.
The detector converts the resulting interference (equation 2.12) into a voltage signal. This signal is then amplified and measured via an oscilloscope. A PC uses a Local Area Network (LAN) connection to retrieve the measurement data from the oscilloscope. This allows us to compare the frequency of the coherent light of our standalone stabilized He-Ne laser source with the frequency of the coherent light of another laser source.

To describe the dynamic behaviour of our implemented control algorithm, we use the I/O interface and a DAQ to measure the intensity of the axial modes of the standalone stabilized He-Ne laser source.

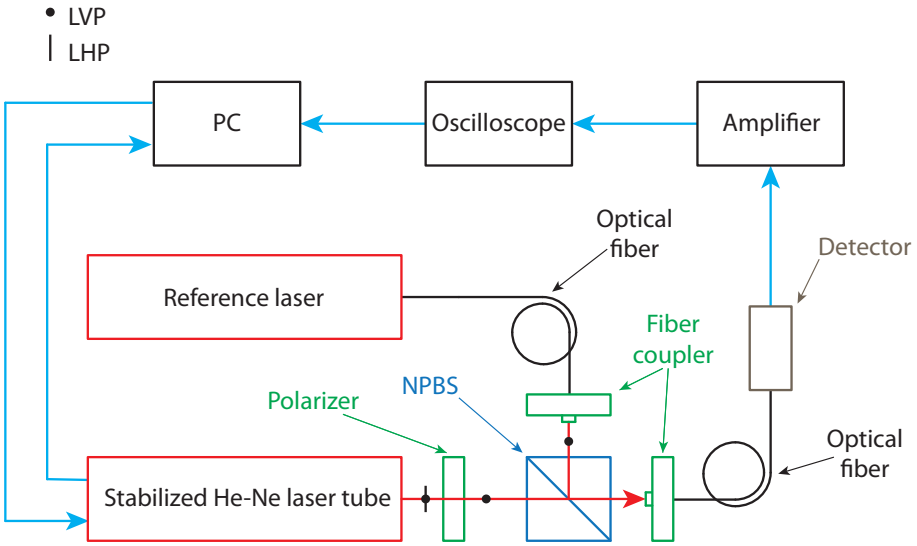

Figure 6.1: The measurement assembly which we use to determine the frequency stability of the standalone stabilized He-Ne laser source. The underlying principle is the heterodyne detection.

6.1.1 Components

This subsection describes the major components which we use in the measurement assembly.

Detector

To measure the intensity of the incident light we use one DET02AFC Fiber Input Si Photodetector from Thorlabs [37] with the following specifications.

- It produces an output voltage (V_{out}), at a load resistance of 50 Ω, between 0 to 410 mV depending on the intensity of the incident light.
- It has a bandwidth of 1.2 GHz.
- The wavelength range is between 400 nm and 1100 nm.

Amplifier

To amplify the weak voltage signal from the detector we use the 310 low noise amplifier from Sonoma [35]. It provides a bandwidth of 9 kHz – 1 GHz and a gain of 32 ± 1.5 dB.

Oscilloscope

To sample the amplified voltage signal we use the TDS7154B Digital Phosphor Oscilloscope from Tektronix it holds four 8-bit input channels with a bandwidth of 1.5 GHz and a 20 GS/s sampling rate.

6.2 Frequency Stability of the Standalone Stabilized He-Ne Laser Source

We measure the frequency stability of our standalone stabilized He-Ne laser source, by comparing it to the SL-03 He-Ne laser from SIOS [33]. We use the TDS7154B oscilloscope to sample the amplified voltage signal with a sample rate of 250 MHz and retrieve a data vector of 10000 samples. We analyze the data using Matlab™7.10.0. The developed algorithm works as follows.

- Missing data vectors are discarded. This concerns $< 0.1\,\%$ of the data vectors.
- We estimate for each data vector the Power Spectral Density (PSD) using the Matlab™function *pwelch()* [20]. This function splits the data vector into eight, 50 % overlapping, segments. It applies a hamming window to each segment and uses an N-point Fast Fourier Transformation (FFT) to compute a modified periodogram. Finally the set of modified periodograms is averaged and scaled with the sampling frequency.
  The frequency resolution equals the main lobe width of the applied window. We calculate for a 2222-point Hamming window (given by a data vector of 10000 samples, 8 segments with 50 % overlap) a main lobe width (-3 dB) and, therefore, a frequency resolution of 0.14 MHz. We interpret this frequency resolution as a quantization with a quantization error of ± 0.05 MHz.
- We analyze the PSD regarding its maximum. Figure 6.2 shows a PSD of one data vector. We see that the PSD contains very high noise components. This is caused by the amplifier in our measurement assembly. Therefore, we are only able to analyze a certain area of the spectrum. This area is also depicted in figure 6.2.
  This has no effect on the reliability of the measurement, since we are able to move the beat frequency in the spectrum. We simply change the frequency of our stabilized He-Ne laser source and, therefore, change the frequency of the beat frequency. This is done by changing the reference variable.
- After we check every PSD for the beat frequency, we write the corresponding value into a new vector. This vector now represents the measurements of the beat frequencies for a sample time of one second.

For reasons we discuss in section 2.3, we express the frequency stability with the overlapping ADEV. To compute the overlapping ADEV we use the Matlab™function *allan_overlap() v2.22* [15]. This function calculates the overlapping ADEV for a given frequency

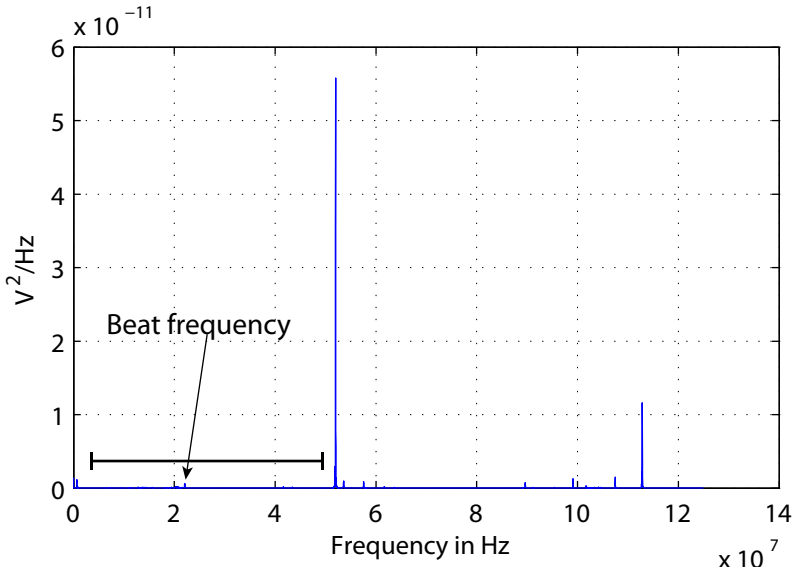

Figure 6.2: The PSD of one data vector. The high noise components limit us to analyze only a certain area of the spectrum.

vector and sample time for given time intervals (τ). It also plots the corresponding sigma-tau diagram.
In addition we also state the frequency stability in ppb. We do this because the stability of the reference laser is also expressed in ppb. Therefore, we calculate the maximum frequency variation

$$\delta f_{Beat} = max(f_{Beat}) - mean(f_{Beat}), \tag{6.1}$$

where $max(f_{Beat})$ is the maximum beat frequency and $mean(f_{Beat})$ is the mean beat frequency. We relate this result with the nominal frequency (473,612,392.985 MHz [31]) of the reference laser.

In the following two subsections we will discuss two experiments we perform to characterize the stability of the measured beat frequency. Since the frequency stability of the reference laser is not high enough (according the test certificate ±20 ppb [31]), we cannot state that our stabilized He-Ne laser source accounts for almost all the ADEV. The results are influenced by frequency variations in both laser sources.

6.2.1 Stability of the Beat Frequency without Disturbances

This experiment aims to test the frequency stability of the beat frequency under conditions as we expect them in any optical metrology laboratory. This means that we keep the doors

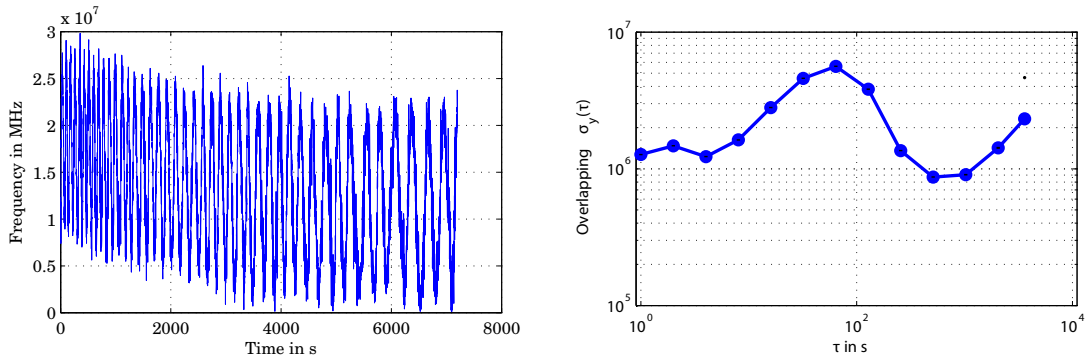

(a) (b)

Figure 6.3: The behaviour of the measured beat frequency over two hours without disturbance present. The beat frequency versus time (a) and the sigma-tau plot of the calculated overlapping ADEV (b).

and windows shut to avoid any rapid change in temperature and pressure of the ambient air. And we also try to avoid disturbances caused through mechanical vibrations.
We measure for a period of two hours after both laser sources are in operation for at least 2 hours. To positon the beat frequency in the area where no high noise is present, we set the reference variable to $r = -3$.

Figure 6.3(a) plots the beat frequency versus the measurement time, figure 6.3(b) shows the sigma-tau diagram of the overlapping ADEV. The sigma-tau plot shows the graphic context of the calculated overlapping ADEV values, as they are summarized in table 6.1.

τ in s	1	2	4	8	16	32	64	128	256	512	1024	2048
$\sigma_y(\tau)$ in MHz	1.3	1.5	1.2	1.6	2.8	4.6	5.6	3.8	1.4	0.9	0.9	1.4

Table 6.1: The calculated values of the overlapping ADEV without disturbance present.

The long term drift in the frequency is typical for a He-Ne laser during its first hours of operation. The reason for the midterm variations of the frequency, however, is unknown. We never experience such a behaviour in the experiments we make in chapter 4.

Using equation 6.1 we obtain a maximum frequency variation, measured over one hour, of ± 31 ppb. This result is very satisfactory, since the stability of the reference laser is stated with ± 20 ppb.

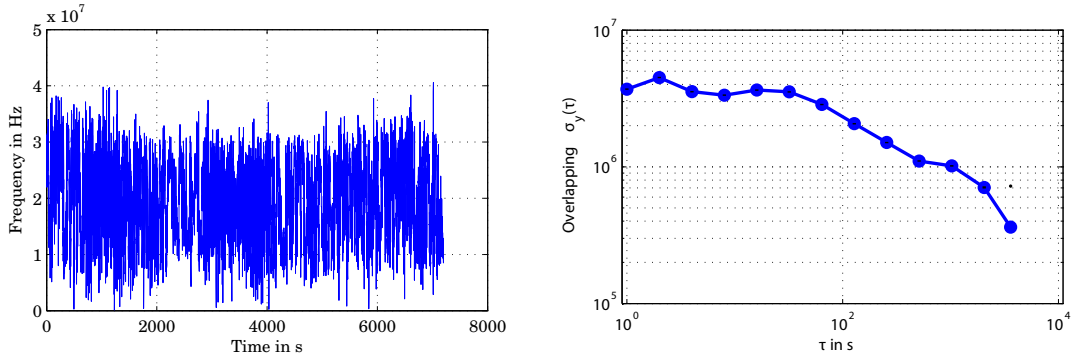

(a) (b)

Figure 6.4: The behaviour of the measured beat frequency over two hours with disturbance present. The beat frequency versus time (a) and the sigma-tau plot of the calculated overlapping ADEV (b).

6.2.2 Stability of the Beat Frequency with Disturbances

In the next experiment we test the stability of the beat frequency under the influence of disturbance. Therefore, we open one window and the opposing door of the laboratory, to create an airflow around the stabilized He-Ne laser source.
Again we measure for a period of two hours after both laser sources are in operation for at least 4 hours. In this measurement the noise makes it necessary to set the reference variable to $r = -2.5$.

The results are depicted in figure 6.4(a), figure 6.4(b) and table 6.2. Contrary to the first measurement is that the short term frequency fluctuations are much higher. This is expected, because the rapid changes in pressure and temperature forces the controller to permanently adjust the controlled variable. The long term drift is no longer present which indicates that after 4 hours the stabilized He-Ne laser tube has settled down. Again the midterm variations are present.

τ in s	1	2	4	8	16	32	64	128	256	512	1024	2048
$\sigma_y(\tau)$ in MHz	3.7	4.5	3.5	3.3	3.6	3.5	2.9	2.1	1.5	1.1	1.0	0.7

Table 6.2: The calculated values of the overlapping ADEV without disturbance present.

Using equation 6.1 we obtain a maximum frequency variation, measured over one hour, of $\pm 42\,\text{ppb}$.

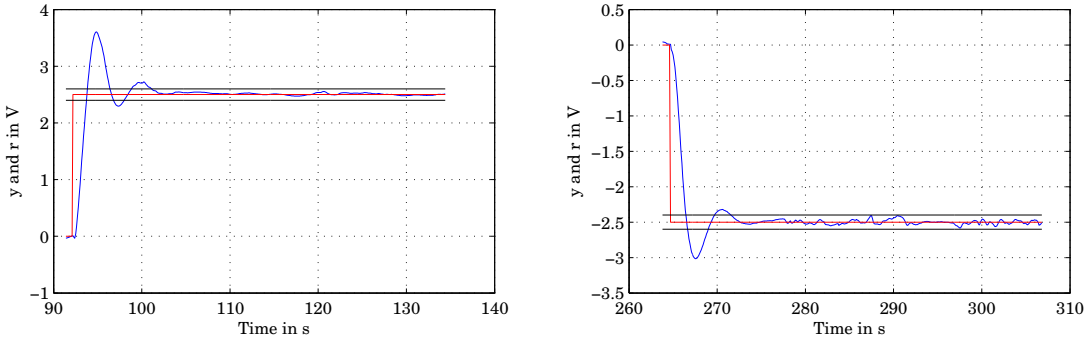

(a) (b)

Figure 6.5: Two performed steps in the reference variable and the error band ($\epsilon = \pm 0.1$). (a) $r = 2.5$ and (b) $r = -2.5$

6.3 Dynamic Behaviour of the Standalone Stabilized He-Ne Laser Source

In this experiment we investigate the time response of the closed control loop of our stabilized He-Ne laser tube regarding the rise time t_r, settling time t_s (for $\epsilon < \pm 0.1$), delay time t_d and the overshoot expressed as percentage.

To measure the exact relation between the reference r and control variable y, we make use of the external controller function of our MCU. This means that we sample the detector signals from the I/O interface using the previous described DAQ, calculate the PI controller with a PC and feed the calculated manipulated variable via the I/O interface back to the MCU. Because we use the same sampling rate and controller parameters we expect the same behaviour of the control loop.

We preheat the stabilized He-Ne laser tube to its operating temperature of 80 °C and perform two steps of the reference variable, to $r = 2.5$ and $r = -2.5$. We choose this values because the MCU performs these steps whenever it changes to LHP or LVP mode.
The results are depicted in figure 6.5 and in table 6.3. It is obvious that the behaviour for a positive step of the reference variable differs from a negative step in the reference variable. The reason for this behaviour is that the PI controller reacts on positive control deviations with an increase in heat and on negative control deviations with a decrease in heat. The different behaviour of the step response origins, therefore, in the different dynamics of the heating process and cool down process.

Specification	$r = 2.5$	$r = -2.5$
Rise time (t_r)	1.2 s	1.4 s
Settling time (t_s)	9 s	7.1 s
Delay time (t_d)	0.3 s	0.1 s
Overshoot	44.2 %	20.6 %

Table 6.3: The obtained specifications of the control loop.

6.4 Improvement Possibilities

This section discusses both the improvements possibilities regarding the frequency stability measurements and how to improve the stability of the stabilized He-Ne laser source.

- The measurement assembly is unsatisfactory. Because of the components available, it is only possible to measure a voltage signal with a very low signal to noise ratio. Therefore, we can only search in certain regions of the PSD for the beat signal. This makes the measurement not less reliable but we are not able to measure the warmup behaviour of our stabilized He-Ne laser tube. An improvement of the measurement electronics removes this problem.
- The execution of the measurement is partially unsatisfactory. Unfortunately we are limited to a frequency measurement interval of $\tau = 1\,\mathrm{s}$, a smaller measurement interval is desirable. Besides we experience data loss of $< 0.1\%$. These problems can also be solved by using a better data acquisition.
- Due to the fact that the frequency stability, of the reference laser source is not sufficiently high it is impossible to make reliable statements regarding the frequency stability of our stabilized He-Ne laser source. To properly characterize the frequency stability of our He-Ne laser tube it has to be compared to a reference laser source with much higher frequency stability, e.g. a iodine-stabilized He-Ne laser.
- It is not possible for us to determine the cause of the midterm drift of the measured beat frequency. We suspect that one of the minor changes in the assembly is responsible. The power supply of the He-Ne laser tube uses different ballast resistors. Instead of using duct tape to fix the heating wire we glued in to the surface. It is also possible that some unknown physical effect in the gain medium is responsible or that the He-Ne laser tube reaches the end of its life expectancy.
- As described in section 4.2.2, the available LGR-7641 He-Ne tubes have a non proportional behaviour between the intensity of the waste beam and the output

beam. We remove this problem by putting a drop of epoxy on the outer surface of the HR-mirror. Although the results are satisfactory, it is interesting to know if the frequency stability can be increased by using another He-Ne laser tube which does not have this behaviour. Since our developed hardware is very adaptable, it is no problem to change the existing LGR-7641 He-Ne laser tube for an alternative He-Ne laser tube.

6.5 Summary

This section describes the measurement assembly which we build to compare the frequency of our standalone stabilized He-Ne laser source with the frequency of a reference laser source and it described the major components used in this assembly.
Furthermore it deals with the experiments conducted to characterize the frequency stability and the dynamic behaviour of our standalone stabilized He-Ne laser source. The measured overlapping ADEV for a measurement interval of one second is $\sigma_y(1\,\mathrm{s}) = 1.3\,\mathrm{MHz}$ without disturbance present and $\sigma_y(1\,\mathrm{s}) = 3.7\,\mathrm{MHz}$ with disturbance present.
The section concludes with improvement possibilities both regarding the measurement assembly and the standalone stabilized He-Ne laser source.

7 Conclusions and Outlook

This Diploma thesis deals with the design, implementation, and experimental validation of a two frequency standalone stabilized He-Ne laser source. Based on the requirements, stated in chapter 1, we explain the basic theoretical background necessary to follow the thesis. We analyze and compare three well established methods (Zeeman splitting, comparison of axial modes and Acousto-optic modulator) to stabilize a He-Ne laser tube. Based on this analysis we chose the comparison of axial modes method, since it requires the least complex assembly. Furthermore we describe a method to validate and express the frequency stability of a laser source.
In chapter 4 we test the applicability of the available Siemens LGR-7641 He-Ne laser tubes for the chosen method using an experimental assembly. Therefore, we check for constant polarization states in the emitted coherent light and the proportionality between the intensity of the waste and output beam. Finally we implement a control algorithm.
In chapter 5 we use the obtained knowledge to build a two frequency standalone stabilized He-Ne laser source. In the final chapter we try to validate its frequency stability by comparing it to a reference laser source. We measure a frequency stability, for an averaging time of one second, expressed through the overlapping ADEV of $\sigma_y(1\,\mathrm{s}) = 1.3\,\mathrm{MHz}$. And a maximum frequency variation, measured over one hour, of $\pm 31\,\mathrm{ppb}$. Unfortunately, the stability of the reference laser source is not high enough to provide an accurate estimate of the stability of our standalone stabilized He-Ne laser source.
The task of future student projects has to be the accurate validation of the frequency stability of the standalone stabilized He-Ne laser source and its integration in a heterodyne or homodyne MI.

Appendix

I/O-Panel

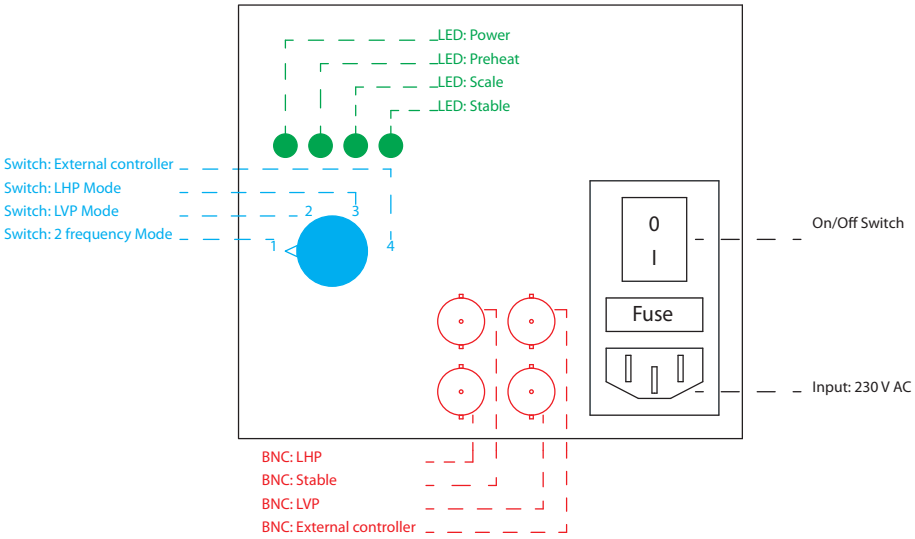

Figure A.1: Schematic of the I/O-Panel on the rear of the hosing.

BNC: External controller

The input $0-5\,\mathrm{V}$ signal is sampled by the MCU and applied, via the PWM, to the heating wire. $0-5\,\mathrm{V}$ equals $0-100\,\%$ of the duty cycle of the PWM

BNC: LVP

Outputs the intensity of the LVP axial mode as a $0-5\,\mathrm{V}$ signal.

BNC: Stable

Outputs $5\,\mathrm{V}$, when the control deviation is within an error band of $\epsilon \pm 0.1$.

BNC: LHP

Outputs the intensity of the LHP axial mode as a $0-5\,\mathrm{V}$ signal.

LED: Stable

Is set when the absolute value of the control deviation is beneath 0.1.

LED: Scale

Is set when the control algorithm is in scaling mode. In this mode the control algorithm forces a fast mode sweep and determines the minima and maxima of the intensities of the axial modes in order to scale them to a maximum of 4. This mode is called only once and lasts 20 seconds.

LED: Preheat

Is set when the controller is in preheat mode. The control algorithm preheats the He-Ne laser tube to its pre set operating temperature.

LED: Power

Is set when the MCU is active. Toggles when the MCU detects intensity signals, from the axial modes, that are too weak.

Overheat

LED: Preheat, LED: Scale and LED: Power is set. The temperature is higher than 120 °C. The PWM is set to zero until the temperature reaches 55 °C.

Switch: 2 frequency Mode

The control algorithm scales the intensity of the two axial modes for 20 seconds. It preheats the He-Ne laser tube to operating temperature and activates the PI-controller. The reverence variable is set so that the emitted coherent light consists of two axial modes with equal intensity.

Switch: LVP Mode

The control algorithm scales the intensity of the two axial modes for 20 seconds. It preheats the He-Ne laser tube to operating temperature and activates the PI-controller. The reverence variable is set so that the emitted coherent light consists of two axial modes, where the LVP axial mode has a higher intensity.

Switch: LHP Mode

The control algorithm scales the intensity of the two axial modes for 20 seconds. It preheats the He-Ne laser tube to operating temperature and activates the PI-controller. The reverence variable is set so that the emitted coherent light consists of two axial modes, where the LHP axial mode has a higher intensity.

Switch: External controller

The input $0-5\,\mathrm{V}$ signal is sampled by the MCU and applied, via the PWM, to the heating wire. If no voltage signal is applied the He-Ne laser tube runs without stabilization.

Circuit diagrams

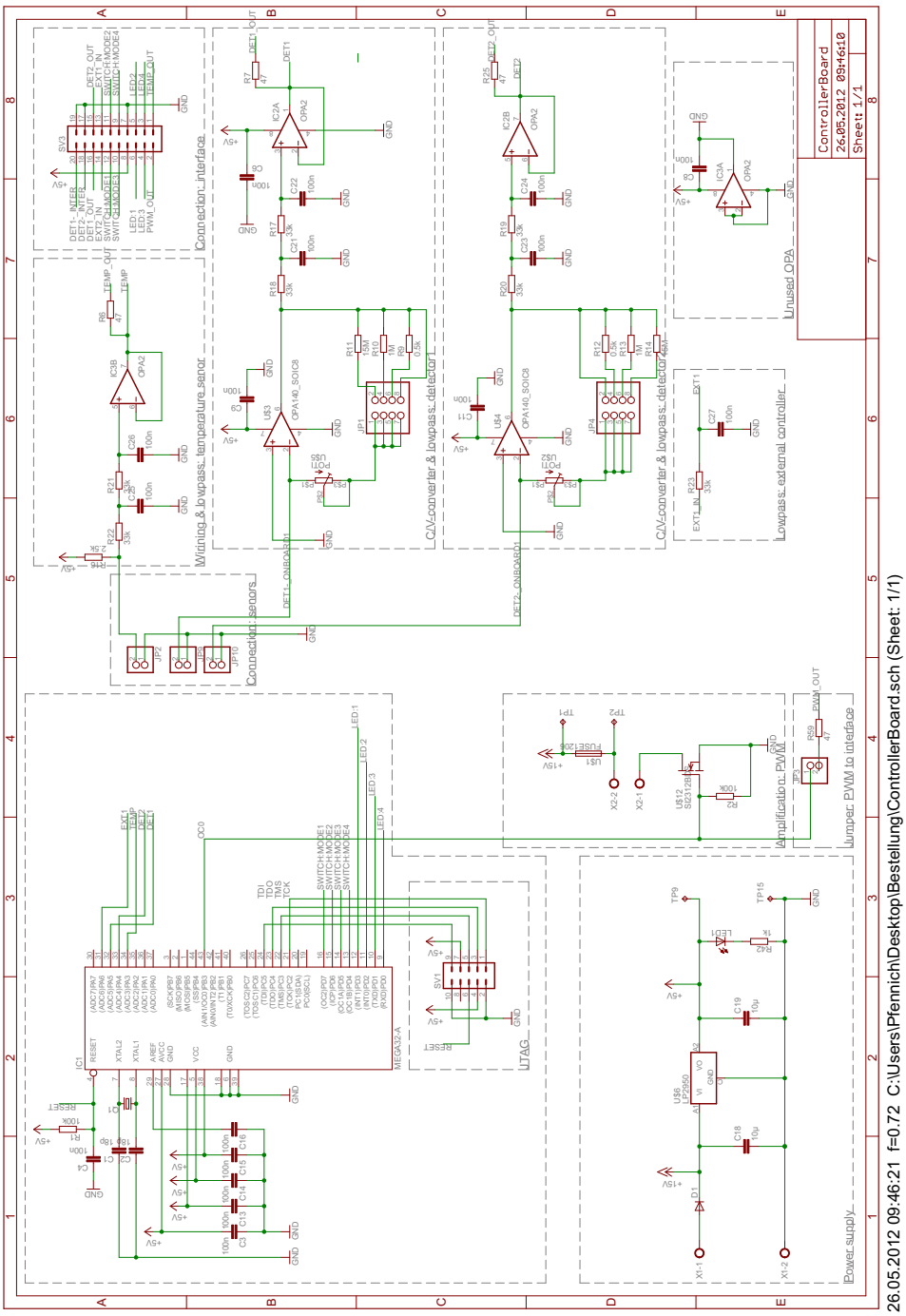

Figure A.2: The circuit diagram of the controller board.

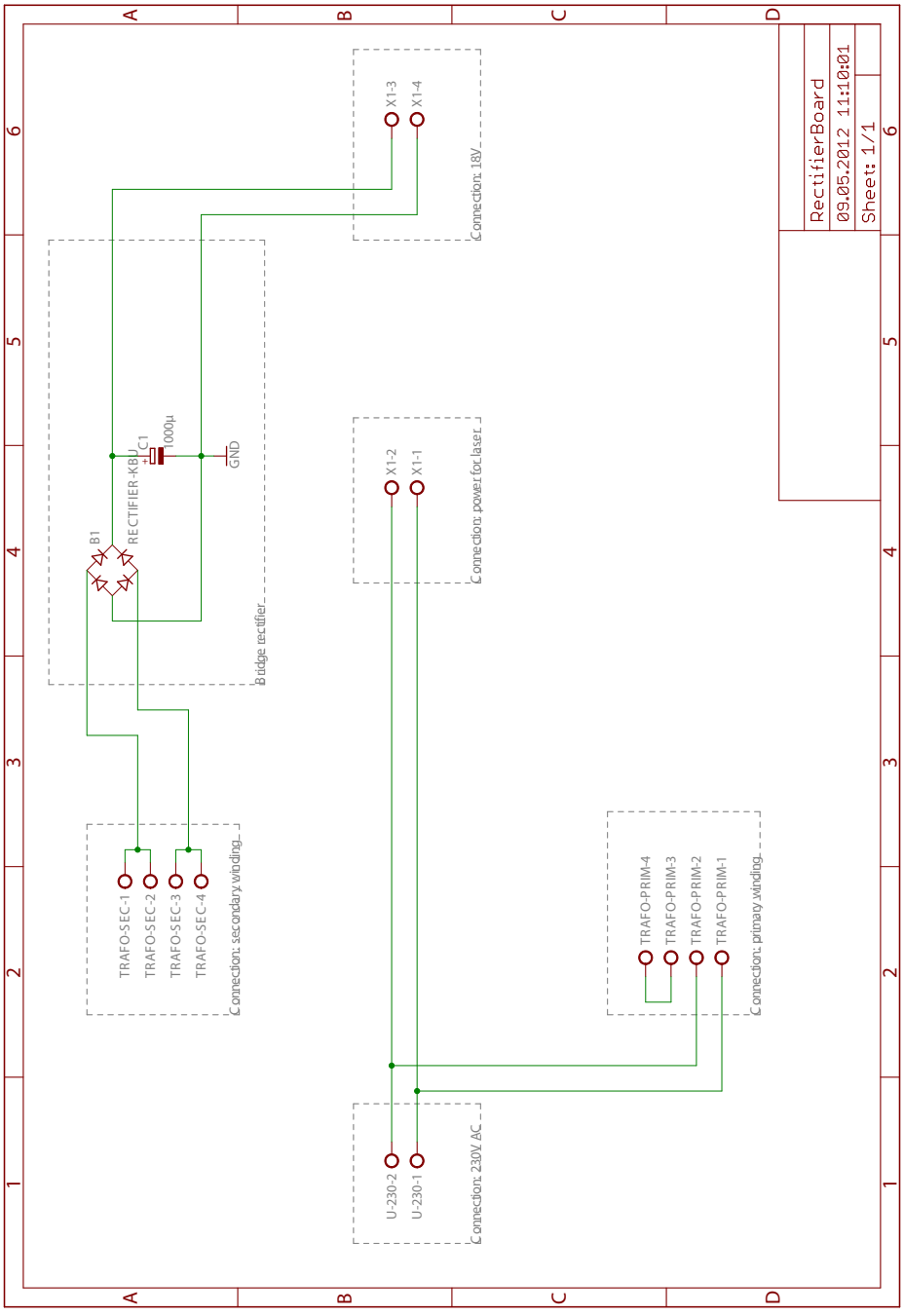

Figure A.3: The circuit diagram of the power supply board.

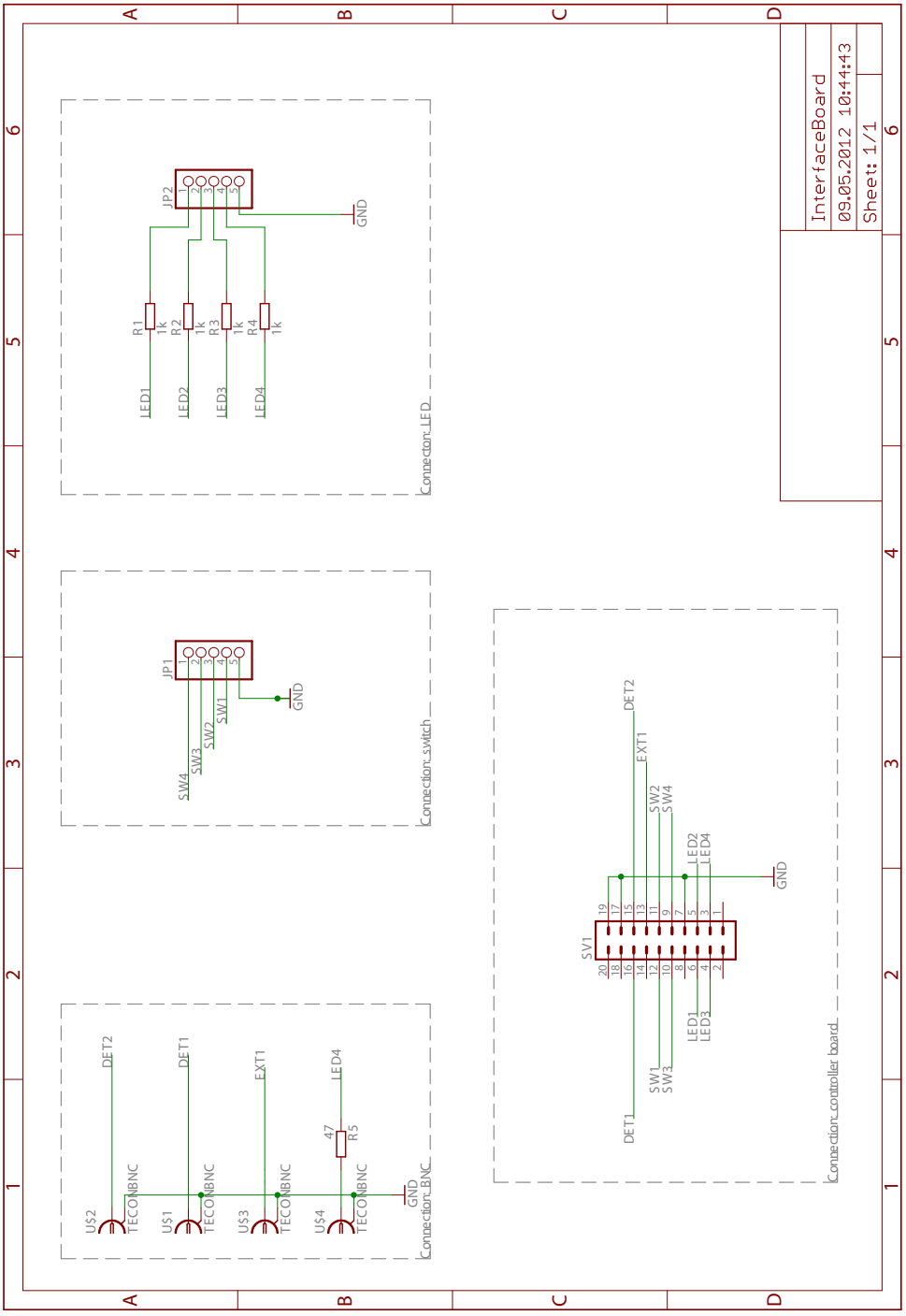

Figure A.4: The circuit diagram of the I/O board.

Design drawings

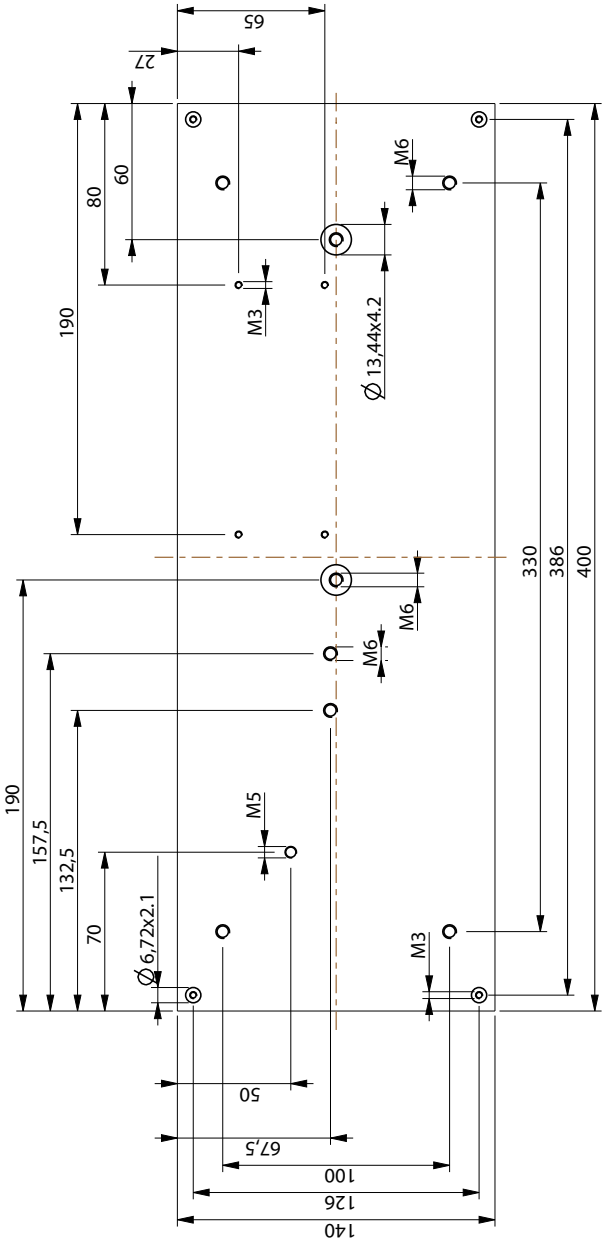

Figure A.5: Design drawing of the baseplate. It is a 8 mm aluminium plate.

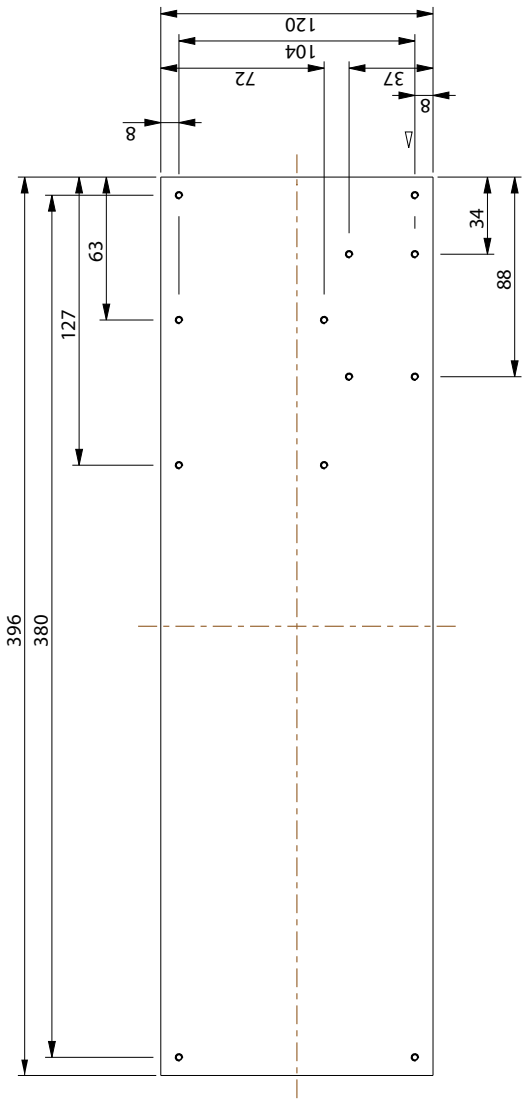

Figure A.6: Design drawing of the side panel. It is a 2 mm aluminium plate. All drills are M3.

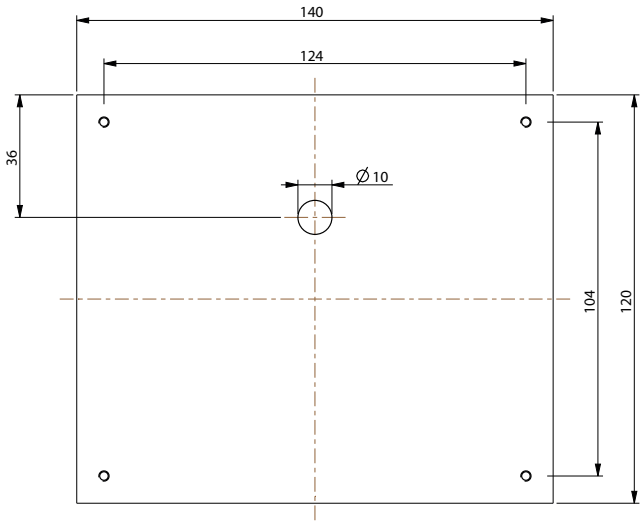

Figure A.7: Design drawing of the front panel. It is a 2 mm aluminium plate.

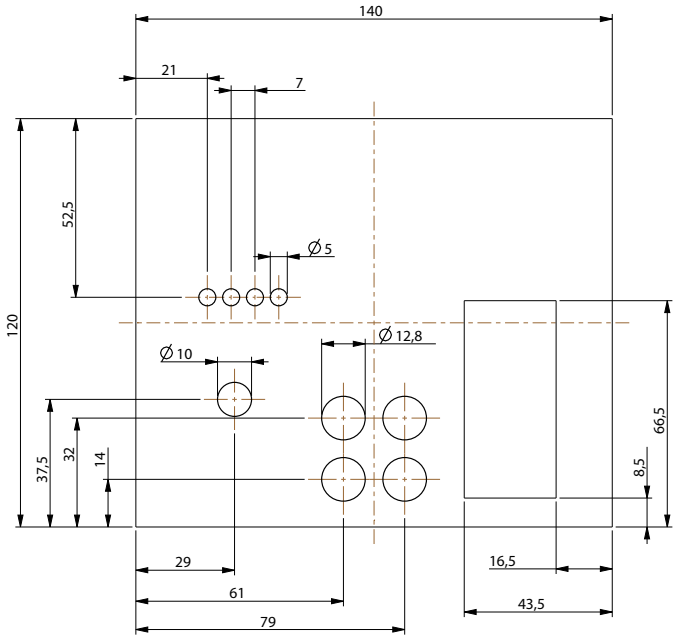

Figure A.8: Design drawing of the rear panel. It is a 2 mm aluminium plate.

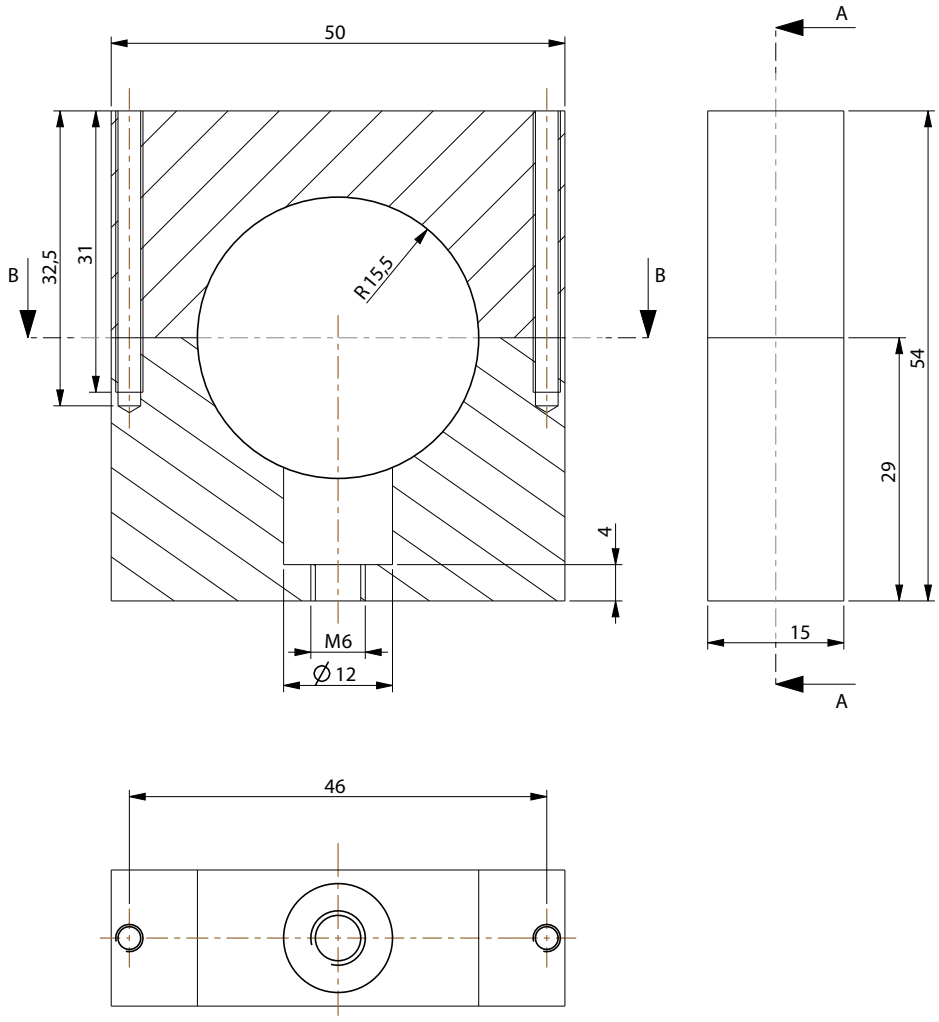

Figure A.9: Design drawing of the front mount of the He-Ne laser tube.

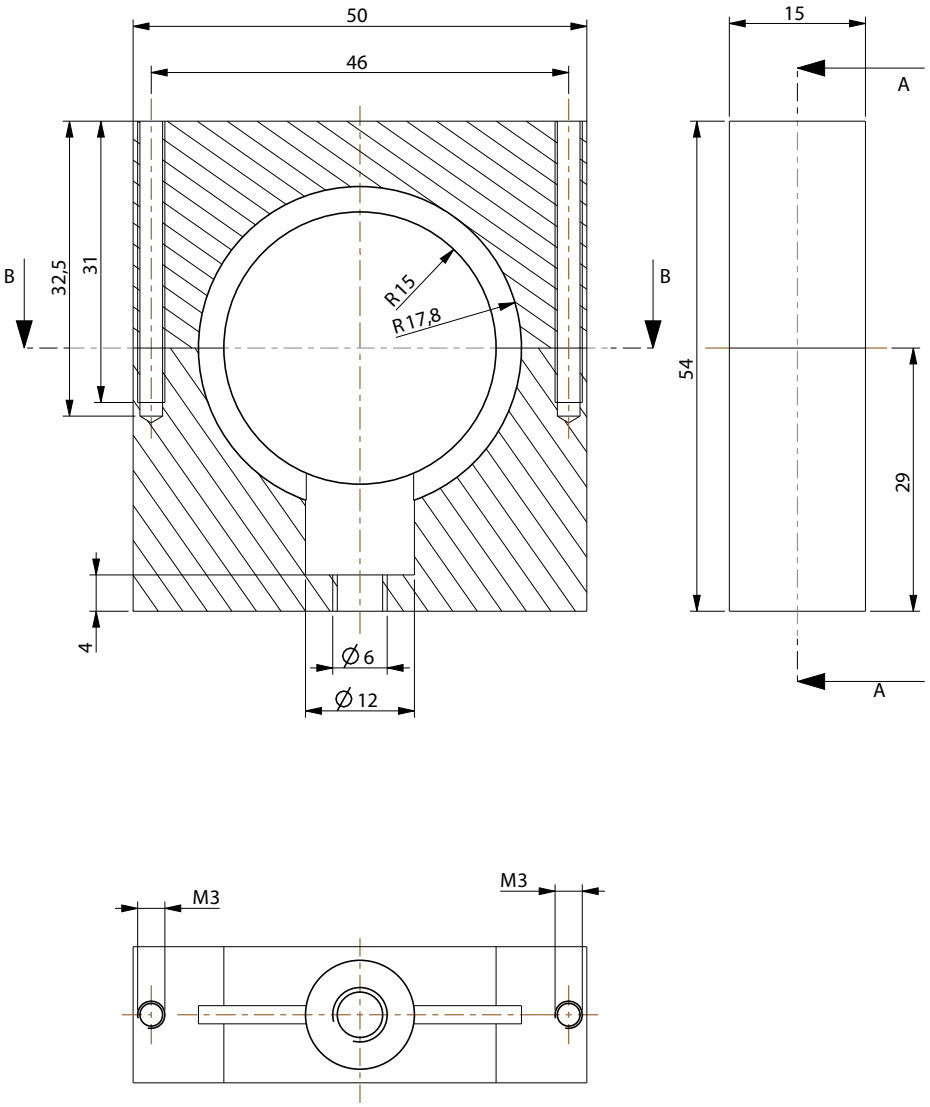

Figure A.10: Design drawing of the rear mount of the He-Ne laser tube.

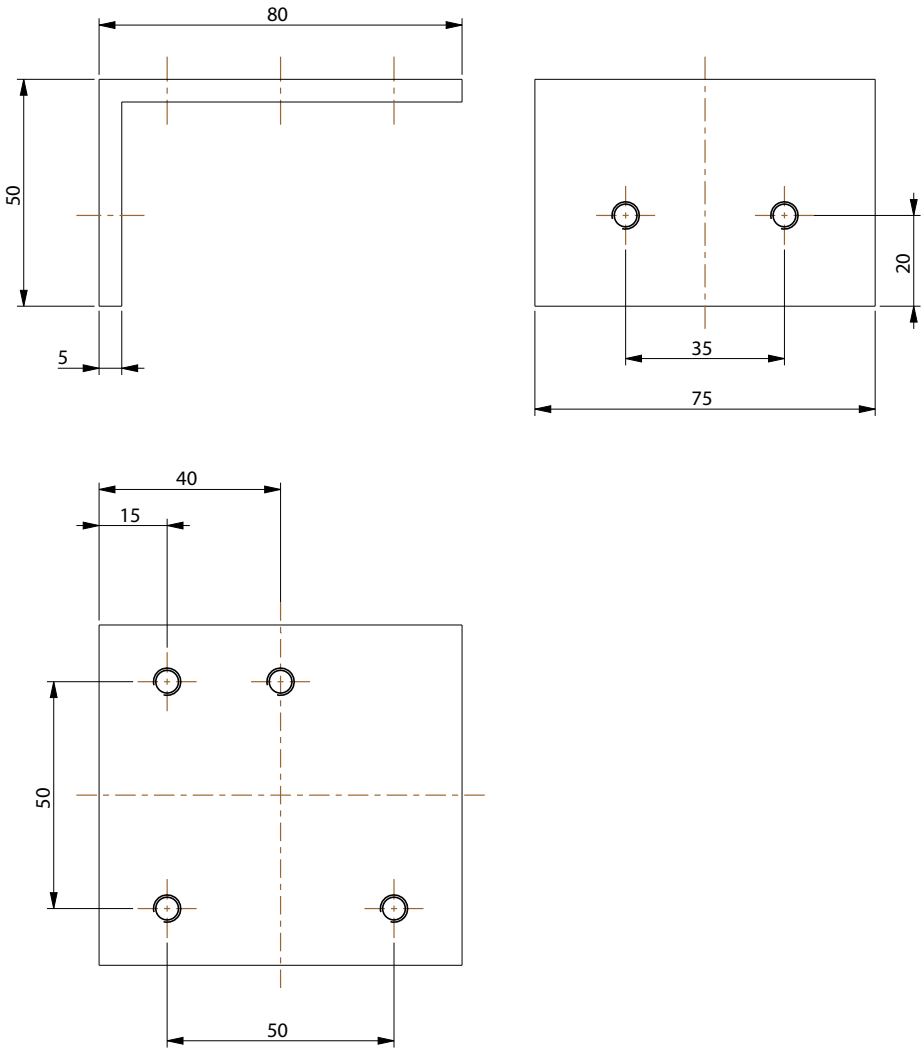

Figure A.11: Design drawing of upper corner plate.

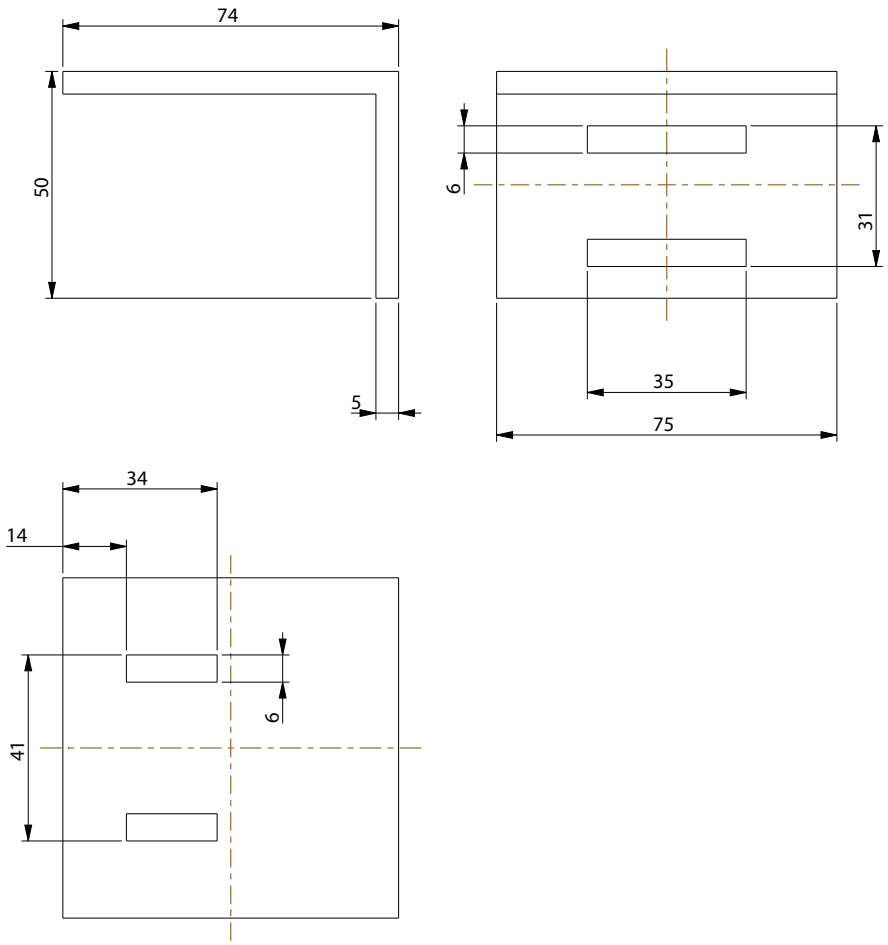

Figure A.12: Design drawing of lower corner plate.

Acronyms

AAF	Anti aliasing filter
AC	Alternating Current
ADC	Analog Digital Converter
ADEV	Allan Deviation
AOM	Acousto Optic Modulator
AVAR	Allan Variance
BNC	Bayonet Neill Concelman
C/V	Current to Voltage
DAQ	Data Acquisition System
DAC	Digital Analog Converter
DC	Direct Current
EMT	Institute of Electrical Measurement and Measurement Signal Processing
FFT	Fast Fourier Transformation
FSR	Free Spectral Range
FWHM	Full Width at Half Maximum
He-Ne	Helium Neon
HR	Highly Reflecting
I/O	Input/Output
JTAG	Joint Test Action Group
LAN	Local Area Network
LCP	Left Circularly Polarized

LED	Light Emitting Diode
LHP	Linearly Horizontally Polarized
LP	Linearly Polarized
LVP	Linearly Vertically Polarized
MCU	Microcontroller Unit
MI	Michelson Interferometer
MOSFET	Metal Oxide Semiconductor Field Effect Transistor
NPBS	Non Polarizing Beam Splitter
NP	Non Polarized
PBS	Polarizing Beam Splitter
PC	Personal Computer
PI	Proportional Integral
ppb	parts per billion
ppm	parts per million
PSD	Power Spectral Density
PWM	Pulse Width Modulation
RCP	Right Circularly Polarized
WSP	Wollaston Prism

Bibliography

[1] AGILENT TECHNOLOGIES. http://www.agilent.com, April 2012.

[2] ATMEL. *ATMEGA32*, April 2012. Data sheet.

[3] AUER M. Untersuchungen zur Messunsicherheit eines Michelson-Interferometers. Technische Universität Graz, 2010.

[4] AUER M. Hochauflösende optische Wegmessung. Master's thesis, Technische Universität Graz, 2011.

[5] BAER T., KOWALSKI F. V. AND HALL J. L. Frequency Stabilization of a 0.633-um He-Ne longitudinal Zeeman laser. *Applied Optics 19 (18)* (1980), 3173–3177.

[6] BALHORN R., KUNZMANN H. AND LEBOWSKY F. Frequency Stabilization of Internal-Mirror Helium -Neon Lasers. *Applied Optics 11 (4)* (1972), 742–744.

[7] CHAPMAN M. Homodyne and heterodyne interferometry. http://resources.renishaw.com/, April 2012.

[8] DIRKSEN P., WERF J. AND BARDOEL W. Novel two-frequency laser. *Precision Engineering 17* (1995), 114–116.

[9] DREVER R. W. P., HALL J. L., KOWALSKI F. V. Laser phase and frequency stabilization using an optical resonator. *Applied Physics B 31* (1983), 97–105.

[10] EICHLER J. UND EICHLER H. J. *Laser Bauformen, Strahlführung, Anwendungen*, 7 ed. SpringerLink, 2010.

[11] ENCYCLOPEDIA OF LASER PHYSICS AND TECHNOLOGY. Acousto-optic Modulators. http://www.rp-photonics.com/acousto_optic_modulators.html, April 2012.

[12] HANSCH T. AND COUILLAUD B. Laser frequency stabilization by polarization spectroscopy of a reflecting reference cavity. *Optics Communications 35 (3)* (1980), 441–444.

[13] HASLE E. K. Polarization properties of He-Ne lasers. *Optics Communications 31 (2)* (1979), 206–210.

[14] HECHT E. *Optik*, 3 ed. Oldenbourg, 1998.

[15] HOPCROFT M. A. *allan_overlap()*, April 2012. Documentation.

[16] HORN M., DOURDOUMAS N. *Regelungstechnik*, 1 ed. Pearson Studium, 2004.

[17] KERN M. Signal Processing for a Homodyne Michelson Interferometer. Master's thesis, Graz University of Technology, 2012.

[18] LAMBDA. *SeriesOMEGA*, April 2012. Data sheet.

[19] LINOS. He-Ne laser. http://www.linos.com/pages/mediabase/original/hne-laser_2492.pdf, April 2012.

[20] MATHWORKS. *pwelch()*, April 2012. Documentation.

[21] NATIONAL INSTRUMENTS. *NI9172*, April 2012. Data sheet.

[22] NATIONAL INSTRUMENTS. *NI9215*, April 2012. Data sheet.

[23] NATIONAL INSTRUMENTS. *NI9263*, April 2012. Data sheet.

[24] NATIONAL INSTRUMENTS. *NI9206*, April 2012. Data sheet.

[25] NATIONAL SEMICONDUCTOR. *LM135/LM235/LM335, LM135A/LM235A/LM335A Precision Temperature Sensors*, April 2012. Data sheet.

[26] NEWPORT. *PBS: 05BC16PC.4*, April 2012. Data sheet.

[27] OSRAM. *Silizium PIN Photodiode BX 65*, April 2012. Data sheet.

[28] RILEY W.J. Handbook of Frequency Stability Analysis. Tech. rep.

[29] SAM'S LASER FAQ. http://www.repairfaq.org/sam/lasersam.htm, April 2012.

[30] SIEGMAN A. *Lasers*, new ed. University Science Books, 1986.

[31] SIOS MESSTECHNIK GMBH. *Werkprüfzeugnis: SL03-L Ser.-Nr.: 181130110*. Test certificate.

[32] SIOS MESSTECHNIK GMBH. http://www.sios.de/, April 2012.

[33] SIOS MESSTECHNIK GMBH. *Stabilized He-Ne Laser SL 03-Series*, April 2012. Data sheet.

[34] SIOS MESSTECHNIK GMBH. *Stabilized He-Ne Laser SL 02-Series*, April 2012. Data sheet.

[35] SONOMA INSTRUMENT. *310 Low Noise Amplifier*, April 2012. Data Sheet.

[36] THORLABS. *DET36A*, April 2012. Data sheet.

[37] THORLABS. *DET02AFC*, April 2012. Data Sheet.

[38] WALLARD A. J. Frequency Stabilization of the He-Ne Laser by Saturated Absorption. *Journal of Physics E: Scientific Instruments 5* (1972), 926–930.

[39] ZYGO CORPORATION. http://www.zygo.com/, April 2012.

[40] ZYGO CORPORATION. Introduction to Displacement Measuring Interferometry, April 2012.